VISION-BASED FOR THE RECOGNITION AND IDENTIFICATION OF THE EDGE OF A TOOTH SAW BUTT JOINT SHAPE

MUHAMMAD SHADIQ BIN LAGANI

UNIVERSITI TEKNIKAL MALAYSIA MELAKA

BACHELOR OF MECHATRONICS ENGINEERING WITH HONOURS
UNIVERSITI TEKNIKAL MALAYSIA MELAKA

2019

VISION-BASED FOR THE RECOGNITION AND IDENTIFICATION OF THE EDGE OF A TOOTH SAW BUTT JOINT SHAPE

MUHAMMAD SHADIQ BIN LAGANI

A report submitted
in partial fulfillment of the requirements for the degree of
Bachelor of Mechatronics Engineering with Honours

Faculty of Electrical Engineering

UNIVERSITI TEKNIKAL MALAYSIA MELAKA

UNIVERSITI TEKNIKAL MALAYSIA MELAKA

2019

DECLARATION

I declare that this thesis entitled "VISION-BASED FOR THE RECOGNITION AND IDENTIFICATION OF THE EDGE OF A TOOTH SAW BUTT JOINT SHAPE" is the result of my own research except as cited in the references. The thesis has not been accepted for any degree and is not concurrently submitted in candidature of any other degree.

Signature : .....

Name : .....

Date : .....

UNIVERSITI TEKNIKAL MALAYSIA MELAKA

APPROVAL

I hereby declare that I have checked this report entitled "VISION-BASED FOR THE RECOGNITION AND IDENTIFICATION OF THE EDGE OF A TOOTH SAW BUTT JOINT SHAPE" and in my opinion, this thesis it complies the partial fulfillment for awarding the award of the degree of Bachelor of Mechatronics Engineering with Honours

Signature : .....

Supervisor Name : .....

Date : .....

UNIVERSITI TEKNIKAL MALAYSIA MELAKA

DEDICATIONS

To my beloved mother and father, the most hardworking and loving people I have ever known.

UNIVERSITI TEKNIKAL MALAYSIA MELAKA

ACKNOWLEDGEMENTS

I wish to express my sincere appreciation to my supervisor, Dr. Hairol Nizam bin Mohd Shah for his continuous encouragement, guidance and support. Without his contributions, this project would not have been completed and presented here. I am also thankful to my panels, Pn. Fadilah binti Abdul Azis and Pn. Norafizah binti Abas for their critic guidance and inputs in polishing this project report.

My gratitude also towards our program coordinator, PM Dr. Ahmad Zaki bin Shukor for his hard work and contributions in ensuring the program always runs smoothly. I am also indebted to Universiti Teknikal Malaysia Melaka (UTeM) for their assistance in supplying the relevant literatures and funding.

My sincere appreciation also extends to all my colleagues and others who have provided assistance at various occasions. Their views and tips are useful indeed. Unfortunately, it is not possible to list all of them in this limited space. Last but not least, my deepest gratitude towards my family for their continuous support and prayers throughout this project completion.

اونيۏرسيتي تيکنيکل مليسيا ملاک
UNIVERSITI TEKNIKAL MALAYSIA MELAKA

ABSTRACT

Nowadays, the most well-known autonomous method in recognizing and identifying the edge of a butt joint implements the usage of vision sensor or laser-assisted vision sensor because of its performance and robustness compared to a manual approach. The most common vision sensors that are used are charge-coupled device (CCD) and complementary metal-oxide semiconductor (CMOS) cameras. This research paper presents the development of a vision-based method to recognize and identify the edge of a tooth saw butt joint shape and evaluation of the accuracy and repeatability of the proposed method. CMOS camera is used in this research because of its high readout speed and inexpensive cost over the CCD camera. The methodology for the digital image processing of the recognition and identification of the edge of a tooth saw butt joint shape comprises of four processes: (1) image pre-processing (2) image segmentation (3) morphological image processing (4) edge butt joint feature points representation and description. The feature points of the edge of a tooth saw butt joint shape which is the start point, supporting point 1 & 2 and the end point is in x and y coordinates of the pixel value image captured by the camera. All the variables in the image processing such as, the threshold values for the edge detection techniques to convert the original image to binary image, the size of the structuring element of the morphological operation dilation and the minimum quality for corner detection is determined and compared to find the most suitable value. The process of the recognition and identification of the edge of a tooth saw butt joint shape is done using different edge detection techniques such as Sobel, Prewitt, Roberts and Canny edge detection technique. The average readings for the feature points is compared to the original points. The comparison shows the accuracy of each method. The average readings are used to calculate standard deviation to show each method's repeatability. The findings suggest that Canny edge detection technique is the most accurate method and all the techniques has a high repeatability due to the reliability of the variables determined and procedures done.

UNIVERSITI TEKNIKAL MALAYSIA MELAKA

ABSTRAK

Pada masa kini, kaedah yang sering digunakan dalam mengenalpasti dan mengiktiraf garisan alur antara dua bahan mengadaptasikan penggunaan sensor penglihatan atau sensor penglihatan dengan bantuan laser disebabkan prestasinya yang tinggi dan binaan yang kuat berbanding kaedah manual. Sensor penglihatan yang sering digunakan ialah kamera peranti pengawal pasangan (CCD) dan semikonduktor logam-oksida pelengkap (CMOS). Kertas penyelidikan ini menerangkan tentang penciptaan kaedah menggunakan sebuah sistem penglihatan untuk mengenalpasti dan mengiktiraf garisan alur antara dua bahan berbentuk gigi gergaji dan membuat penilaian kebolehulangan dan ketepatan terhadap kaedah yang dicadangkan. Kamera CMOS digunakan dalam projek ini disebabkan masa pemprosesan yang cepat dan mempunyai kos yang rendah baik berbanding kamera CCD. Metodologi pemprosesan dalam mengenalpasti dan mengiktiraf garisan alur antara dua bahan berbentuk gigi gergaji terdiri dari empat proses iaitu: (1) pemprosesan imej (2) segmentasi imej (3) pemprosesan imej morfologi (4) mengenal pasti titik kriteria pinggir antara dua bahan berbentuk gigi gergaji. Titik-titik kriteria garisan alur dua bahan berbentuk gigi gergaji dilabelkan "start point", "supporting point 1", "supporting point 2" dan "end point" dalam bentuk koordinat piksel x dan y. Semua pemboleh-ubah seperti dalam proses pemprosesan imej ditentukan dan dibandingkan untuk mencari nilai yang paling tepat. Proses digunakan adalah beberapa teknik seperti Sobel, Prewitt, Roberts Operator dan Canny Edge Detector. Nilai purata dalam bentuk koordinat piksel "start point", "supporting point 1", "supporting point 2" dan "end point" dibandingkan dengan titik sebenar alur bahan bentuk gigi gergaji. Perbandingan tersebut menunjukkan ketepatan setiap satu kaedah yang dilakukan. Nilai purata dari kaedah yang dipilih akan digunakan untuk menunjukkan keboleh-ulangan setiap kaedah tersebut. Kaedah Canny Edge Detection memberi keputusan yang menghampiri bacaan titik-titik kriteria garisan alur tersebut dan kesemua teknik menunjukkan tahap keboleh-ulangan yang tinggi.

UNIVERSITI TEKNIKAL MALAYSIA MELAKA

TABLE OF CONTENTS

UNIVERSITI TEKNIKAL MALAYSIA MELAKA

UNIVERSITI TEKNIKAL MALAYSIA MELAKA

UNIVERSITI TEKNIKAL MALAYSIA MELAKA

LIST OF TABLES

UNIVERSITI TEKNIKAL MALAYSIA MELAKA

UNIVERSITI TEKNIKAL MALAYSIA MELAKA

LIST OF FIGURES

UNIVERSITI TEKNIKAL MALAYSIA MELAKA

UNIVERSITI TEKNIKAL MALAYSIA MELAKA

UNIVERSITI TEKNIKAL MALAYSIA MELAKA

LIST OF APPENDICES

CHAPTER 1

INTRODUCTION

1.1 Overview

This chapter presents the project background on the recognition and identification of the edge of a tooth saw butt joint shape using a vision-based approach, motivation of the project, problem statement that leads to the proposal of the project, objectives as the guideline throughout the project, scope covering the limitation in terms of measurable outcomes and the outline of the project.

1.2 Project Background

The application of a vision-based system in manufacturing industries has increased the productivity, quality control and had given a competitive edge to the industries applying it. The general functions of a vision-based system during manufacturing processes are capturing and acquiring the desired image containing a region of interest for analysis purposes, identifying and describing the distinct features within the region of interest inside the image. The environmental surrounding during the process must be considered in the vision-based system to achieve a consistent outcome. Illumination techniques, for example, structured lighting can be applied to control the environmental surrounding by illuminating the region of interest with uniform illumination. After a proper illumination technique is introduced, image sensing will be the next step to obtain a good quality image. After the image is sensed, digitization will take place in order to convert the image into digital value so it can be read and displayed by machines used in the manufacturing processes. Lastly, digital image processing techniques are used to obtain the desired final image state for the manufacturing processes [1,2].

UNIVERSITI TEKNIKAL MALAYSIA MELAKA

One of the manufacturing activities that apply this technology is metal butt joint recognition or seam weld tracking which commonly seen in robotic welding application [3]. Basically, a butt joint is the union of two materials, which in robotic

welding process, a metal material joined in parallel which forms a discontinuity of boundary between both of the material where the robot will weld it together. There are various butt joint shapes such as straight, curved, tooth saw and et cetera [4]. This discontinuity represents an edge where it can be detected by a vision-based system and represented and described using digital image processing techniques. When the image of the edge is obtained, digital image processing techniques can be applied such as, image segmentation, morphological image processing and representation and description of image. Those techniques can filter the image from unwanted information, such as noise and reflections, convert image to binary image for further analysis and extraction of features, such as the shape of the butt joint respectively [1,2].

In this project, a vision-based approach to recognize and identify the edge of a tooth saw butt joint shape is developed. The image containing the edge of the tooth saw butt joint shape is captured, digitized and processed using digital image processing techniques. The image is segmented and analyzed to extract the tooth saw shape feature in coordinates pixel value. The accuracy and repeatability of the approach will then be tested.

1.3 Motivation

UNIVERSITI TEKNIKAL MALAYSIA MELAKA

The implementation of machine vision in manufacturing processes has become a global trend in the industrial automation due to its beneficial aspect in terms of production and economic benefits. The increasing on high demands in productions and skilled laborers in today's competitive global market also leads to the increase of application of machine vision. By implementing a vision-based system to the machines operated in manufacturing processes, it can reduce the downside of the current manually operated machines [4,5,6].

According to VDMA Machine Vision Association, the sales within the machine vision market in Germany has risen by 8% as of 2016 up to 2.2 billion euros. The graph shows a significant increasing trend from the year 2010 until 2016. The cause of the increasing trend according to [7], is the widespread of machine vision technologies onto new application worldwide. Figure 1.1 shows the graph of German machine vision industry sales [7].

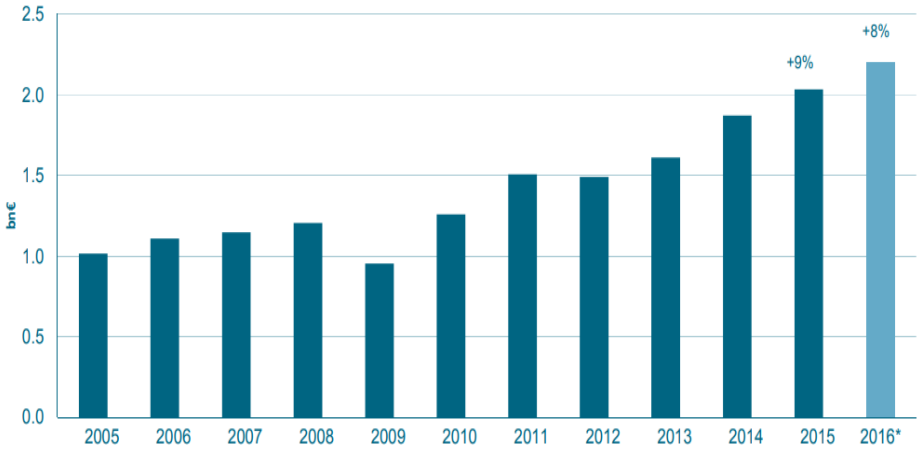

Figure 1.1 German machine vision industry sales [7]

Figure 1.2 shows the customers of VDMA Machine Vision Association based on industries sectors. By evaluating each individual sectors on 2014 and 2015, the VDMA determined that automotive industries are the most common customer with a percentage of 22% of the total earnings. Semiconductor industries is the second common customer, 13% total earnings. Other manufacturing industries has a percentage of 8% out of the total earnings [7].

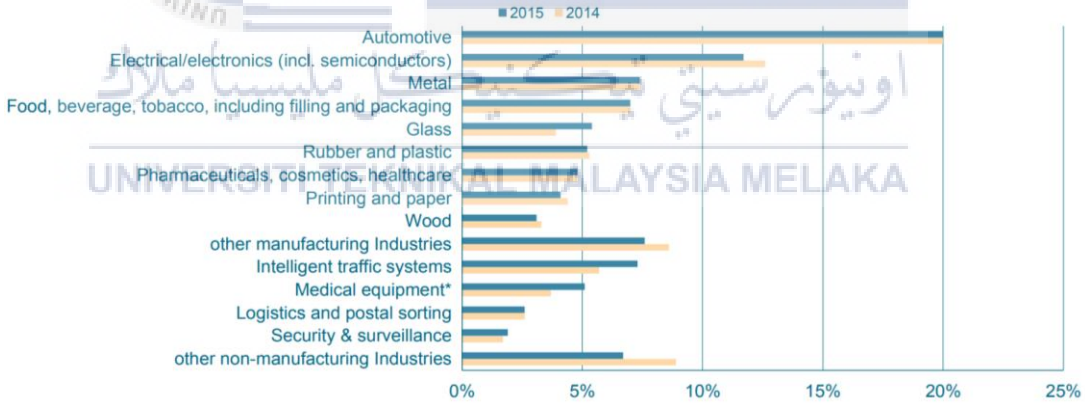

Figure 1.2 VDMA Machine Vision Association customers based on industries section [7]

Machine vision-based system application in manufacturing process which includes the recognition of edge butt joint shape for robotic welding has a proven potential of increasing in terms of economy aspect. The vision-based system aids the robotic welding in identifying its weld seams easily and autonomously.

UNIVERSITI TEKNIKAL MALAYSIA MELAKA

1.4 Problem Statement

Today's current method in recognizing and identifying the edge of a tooth saw butt joint shape in manufacturing processes, mainly in modern robotic welding are using manual operation which is by depending on human observations. The robot is customized and calibrated using "teach and playback" techniques by skilled human operators each time a new edge of tooth saw butt joint shape with different measurements is introduced. Through this repetitive process, it can be time consuming causing the rate of production of the industry using this current method to have a low rate of production. The complexity shape of the edge of a tooth saw butt joint also contribute in the time consumption of operation. It also increases cost to hire several skilled operators to operate the robot manually [4,5,6].

In order to solve the problem, a fundamental machine vision engineering knowledge is required. A vision-based system with good illumination source can be applied to the robotic welding enabling it to recognize and identify the feature points (start, supporting and end) of the edge of the tooth saw butt joint shape automatically. By doing so, the duration of operation in recognition of the edge of the tooth saw butt joint shape will be brief. The implementation of the vision-based system will also reduce the cost required to hire many skilled operators.

UNIVERSITI TEKNIKAL MALAYSIA MELAKA

Digital image processing techniques is required to process the image captured by the vision-based system of the edge of a tooth saw butt joint shape which enables the feature points of the edge of a tooth saw to be extracted. The techniques consist of enhancement, segmentation, edge detection and morphological operation [8]. Hence, through those techniques, the feature points of the edge of a tooth saw butt joint shape can be described and presented.

1.5 Objective

The following objectives serve as a guideline throughout the project. There are four objectives in this project which are:

1. To develop a vision-based method in recognizing the edge of a tooth saw butt joint shape.
2. To identify the feature points of the edge of a tooth saw butt joint shape using vision-based operation.
3. To evaluate the accuracy of the identified feature points compared to its actual feature points.
4. To evaluate the repeatability of the developed method in identifying the feature points of the edge of a tooth saw butt joint shape.

1.6 Scope

This project is done in a controlled environment with only one source of illumination which is a uniform LED light source with a variable brightness of 50, 30 and 10 lumens. The vision sensor used is a CMOS camera with active resolution of 1280 x720 pixels, which is placed in a fixed position, 20 cm vertically from a work piece. The material of the work-piece is made from hard cardboard that is spray painted using silver paint color to imitate the reflection towards light behavior of an aluminum alloy sheet with dimensions 100mm × 100mm × 1mm thickness. A tooth-saw edge shape was cut in the middle of the hard cardboard to imitate an edge of a tooth-saw butt joint shape. The CMOS camera captures the work piece in digital image form which contains the the edge of the tooth saw butt joint shape. The image is then imported, processed and presented using the MATLAB Image Processing Toolbox software to identify feature points, start, supporting 1 & 2 and end points which represents the shape of an edge of a tooth saw butt joint. The methods used in order to detect the edges are Canny, Prewitt, Sobel and Roberts edge detector. The common application of this vision-based system is mostly used in robotic welding operation [3] but, in this project, it only covers until the identification and recognition of the pixel coordinates features of the edge of a tooth saw butt joint shape which will be in x and y axes pixel coordinates. There is no robot path planning for the implementation of robotic welding in this project.

UNIVERSITI TEKNIKAL MALAYSIA MELAKA

1.7 Thesis Overview

This thesis comprises of five chapters. Chapter 1 introduces the project background, motivation, problem statement, objective and scope of this project.

Chapter 2 covers the theoretical background of the types of vision-based sensors, camera, illumination, digital image processing techniques and reviews on past research done by other researchers. This chapter also summarize the research gap based on the past researches.

Chapter 3 discusses the methodology used in the project. This chapter discusses on the experimental setup configuration, the digital image processing techniques used to identify the feature points of the tooth saw butt joint shape and the accuracy and repeatability evaluations.

Chapter 4 explains results and errors that will be obtained from the task and experiments done in Chapter 3 in forms of tables, figures and analysis based on the results obtained.

Chapter 5 concludes the research project that has been done in FYP 1 and FYP 2 and the future work that can be recommended and done in this project.

UNIVERSITI TEKNIKAL MALAYSIA MELAKA

CHAPTER 2

LITERATURE REVIEW

2.1 Overview

This chapter provides a detailed explanation on vision-based sensors for butt joint edge detection including its devices and detection requirements. Having a brief explanation on the fundamentals of digital image processing in recognition and identification of the edge of a tooth saw butt joint shape. Reviews on previous researches and works related to the project are revised and presented on this chapter.

2.2 Vision Sensor

A vision-based sensor to recognize and identify the edge of a butt joint shape are a non-contact type sensor. The most commonly used sensor are vision sensor and laser assisted vision sensor. The general function of a vision sensor is to sense the existence, position and displacement of an object. The configuration of a vision sensor that is used consist of a camera and a filter [3].

UNIVERSITI TEKNIKAL MALAYSIA MELAKA

As for the laser assisted vision sensor, the general function is quite similar to the typical vision sensor, except the configuration of the laser assisted vision contains an extra component which is a laser diode. The sensor is placed with the laser diode at a fixed angle to acquire the projection of laser diode accurately on the work piece. The laser diode produces light strips or light points which will then be examined by the camera. The function of the laser diode is to trace the edge of butt joint and guide the vision sensor along it which enable the vision sensor to identify the discontinuity of the edge of the butt joint with ease. By having the laser diode in assisting the sensor, it helps to reduce the complexity in operating the detection process, thus reducing in time consumption. Table 2.1 shows the summarized comparison between the two sensors based on its advantages and disadvantages [3].

Table 2.1 Comparison between vision sensor and laser assisted vision sensor [3]

Types of Sensor	Advantages	Disadvantages
Vision Sensor	• Easy installation process • Availability • Low cost	• High complexity in calculation
Laser Assisted Vision Sensor	• Minimum margin of error • Simple image processing process. • Wide-range of work piece application (type of material & thickness)	• High cost • High complexity in installation

2.3 Type of Camera

The commonly used camera in the detection of the edge of a butt joint shape, which acts as the vision sensor are Charge-Couple Device (CCD) and Complementary Metal-Oxide Semiconductor camera (CMOS).

2.3.1 Charge-Couple Device (CCD)

The CCD is a vision sensor which is located inside a digital camera. The function of the CCD is to capture an image and transfer it to the camera's memory system and record it as an electronic data. The image contains tiny pixels where, each and one of them corresponds to a single section of the CCD. The CCD is made from several millions of semiconducting silicon which is photosensitive.

It is design as a rectangular shape containing a channel blockade which divides the CCD into rows. Perpendicular to the channel blockade is a thin strips of electrode, commonly made from aluminum to channel the electrical charge. Each pixel is bounded by channel blockade and the electrode which forms a grid of pixels. When it is exposed to any sort of illumination, different segments of the CCD build up electrical charges proportional to the source of illumination intensity. The electrical charge can be measured to obtain a precise information of how bright the section of the image is. The CCD shifts the electrical charges from row to row without using any wires until

UNIVERSITI TEKNIKAL MALAYSIA MELAKA

the charges reach the last row where a readout registers transfer it to the camera's memory. The camera then counts the charges and construct the image using the charges that were converted to electronic data. Figure 2.1 shows the architecture and transfer process of the CCD [9].

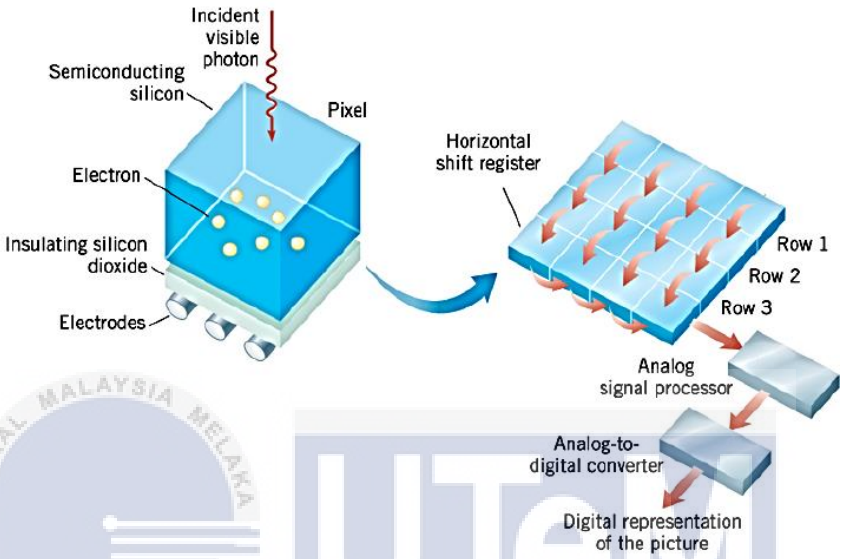

Figure 2.1 Architecure and transfer process of the CCD [9]

2.3.2 Complementary Metal-Oxide Semiconductor (CMOS) Camera

UNIVERSITI TEKNIKAL MALAYSIA MELAKA

The CMOS, same as the CCD, is a vision sensor that is located inside a digital camera. The CMOS sensor contains a pixel array which detects light, where each pixel has a color (red, green & blue) filter. The detected light which is a photonic data is converted into a digital form and then transmitted in an uncompressed format to the camera's memory. The data is then developed into a full-color value on a per pixel basis in order to create a digital image. Figure 2.2 shows the architecture of the CMOS camera [10].

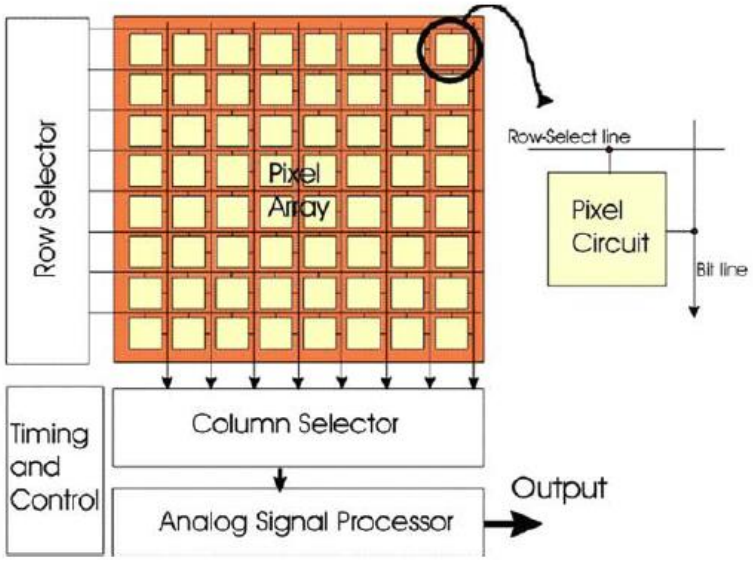

Figure 2.2 Architecture of a CMOS sensor [10]

2.3.3 Comparison between CCD and CMOS Camera

Table 2.2 shows the comparison between the CCD and CMOS sensor based on its advantages and disadvantages.

Table 2.2 Comparison between CCD and CMOS [9,10]

Type of camera	Advantages	Disadvantages
CCD	Superior image quality and flexibility	High power dissipation
CMOS	Superior integration, power dissipation & system size and less expensive	Low image quality

UNIVERSITI TEKNIKAL MALAYSIA MELAKA

2.4 Illumination

In image processing, a constant high quality illumination system is required in order to obtain a good image captured by the camera. By having a good quality image, the process for image analysis will be smooth. There are 5 general types of illumination for digital image processing application which are, LED, metal halide-based (cooled illumination source channeled through fiber-optic cables), laser illumination, fluorescent and halogen illumination. LED illumination has a longer lifespan which can reach up to 50,000 hours, easy to handle, flexibility in its design, low cost and low

power consumption. Basically, a metal halide-based illumination is a combination between the LED illumination and fiber optic illumination. It possesses all the benefits of the LED illumination.

By using a laser illumination combine with a vision sensor, the image analysis will be able to identify depth of an image if the angle between the sensor and work piece is known. Figure 2.3 shows the concept of a laser illumination [11].

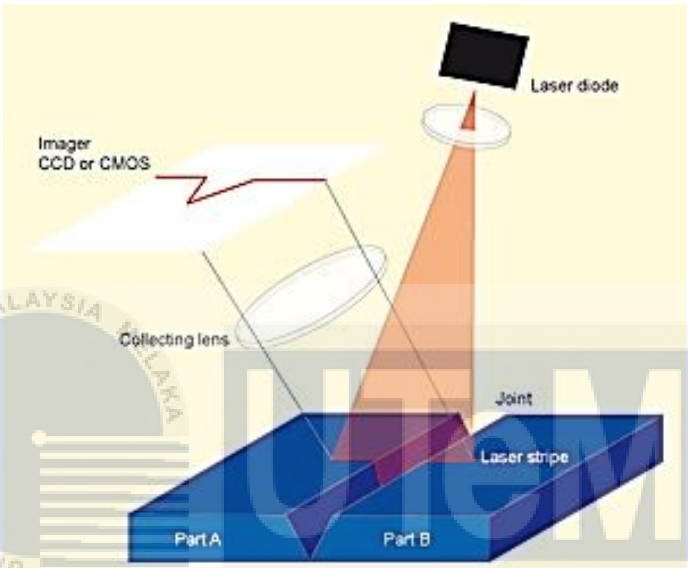

Figure 2.3 Concept of a laser illumination [11]

UNIVERSITI TEKNIKAL MALAYSIA MELAKA

2.5 Digital Image Processing

An image is a two-dimensional representation denoted as a function $f(x, y)$, where x and y is in spatial domain (plane) coordinates and an amplitude of f in any pairing in the spatial domain coordinates of x and y is define as the grayscale or the intensity of an image at coordinates x and y. A digital image is when all of those values has a limit and discrete in values. The study of digital image processing is referring to the processing of these digital images using a digital device. Digital image is a formation of a limited number of elements which has pixel coordinate values. The elements are defined as picture and image elements, pels and pixels. Pixels is the most common terminology used to describe the elements inside a digital image [12].

2.5.1 Morphological Image Processing

Morphological image processing is a set of digital image processing methods which deals with shapes of features in an image. Basically, this operation is applied to remove errors which occurs during image segmentation. This operation is useful for further image processing in the representation and description of a region shape such as discontinuities. This operation simplifies the data from the captured images, keeps distinct shape characteristics and removes noise [13].

2.5.1.1 Dilation and Erosion

Dilation and erosion is a fundamental morphological image processing operations. Both of them are given definitions in terms of more elementary set operations, but commonly used as the fundamental of lots of algorithm. Both of them are formed by the conditions of a set called structuring element with a set of pixels of interest in the image. The structuring element possess a shape and has an origin point. The dilation operation is used for repairing breaks and intrusions. As for erosion, it is used to split apart joined objects and can diminish extrusions. Erosion can be further used for thinning operation where dilation thickens objects in a binary image. Figure 2.4 shows the example of dilation operation and Figure 2.5 shows the example of erosion operation using different size of structuring element [13].

UNIVERSITI TEKNIKAL MALAYSIA MELAKA

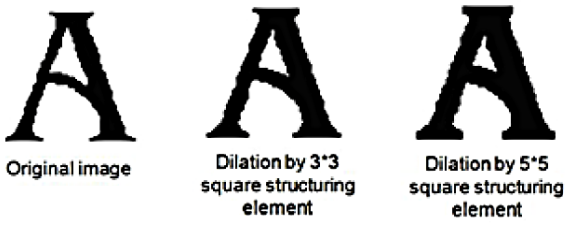

Figure 2.4 Dilation operation [13]

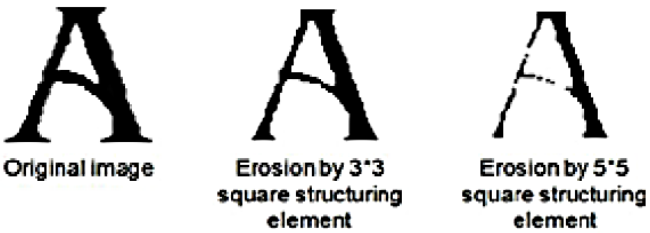

Figure 2.5 Erosion operation [13]

2.5.1.2 Opening and Clossing

The function of opening operation is basically to flatten contoured objects, eliminates narrow edges and reduces thin lumps on the image. For closing, the operation is vice versa to the opening operation. It combines narrow edge and elongate thin gap, removes indistinct crevice and fills up the un-smoothen contour. Figure 2.6 below shows the original image. Figure 2.7 show example of opening operations and Figure 2.8 shows example of closing operations [13].

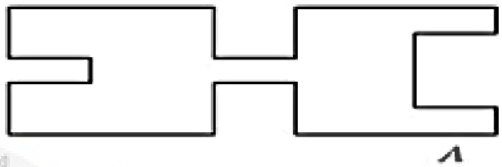

Figure 2.6 Original image [13]

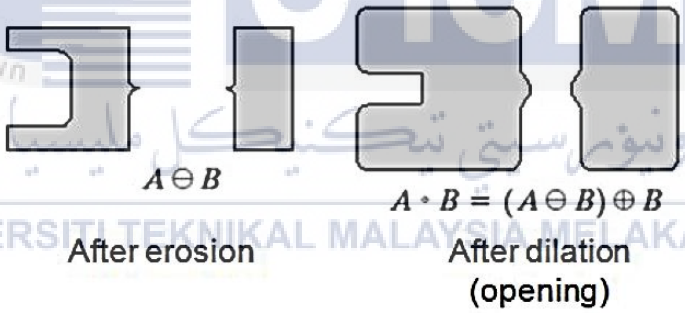

Figure 2.7 Opening operation [13]

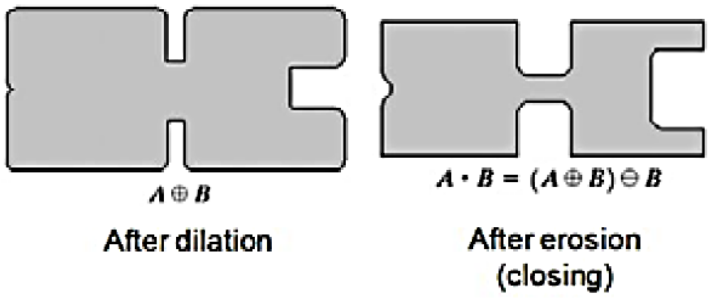

Figure 2.8 Closing operation [13]

UNIVERSITI TEKNIKAL MALAYSIA MELAKA

2.5.2 Image Segmentation

In digital image processing, image segmentation is one of the main procedure in order to do analysis on an image and obtaining documentation in form of data of the image. Image segmentation is a method where image will be divided into parts, which is called segments. The most common usage of image segmentation is in compression of image and recognition and identification of an object inside an image. This is because image segmentation will make the process easy as the process does not require to analyze the whole image, just the partition image that had been segmented. There are several image segmentation techniques, which divides the image into several segments based on the image specific features. Theses image specific features are pixel intensity value, color, contour and et cetera. There several image segmentation techniques such as thresholding, edge detection, spatial based, clustering, watershed, partial differential equation(PDE) based and artificial neural network (ANN) based [14].

2.5.2.1 Thresholding Technique

Thresholding technique is the easiest technique that can be done. This method distinguish the image pixels based on their intensity level on the histogram. This method changes gray images to binary images. The selection of determining the image pixel intensity can be automatic or manual based on its previous image information. A threshold will be set and the condition will be determined whether the image intensity is higher or lower than the threshold. Figure 2.9 shows the example of thresholding technique applied on an image [14].

Figure 2.9 Thresholding from RGB (left) to binary (right) image [14]

UNIVERSITI TEKNIKAL MALAYSIA MELAKA

2.5.2.2 Edge Detection Technique

The edge detection technique is an optimal technique used in digital image processing. This technique detects the abrupt changes in intensity value of groups of pixels in an image which is any discontinuities or boundaries in an image. This technique determines whether the edge intensity is larger than a specific threshold that had been set. This technique will detect the discontinuities inside the image and link it together to form an edge in a region of interest. The basic edge detection techniques operators are Canny, Prewitt, Sobel and Roberts. Figure 2.10 shows the examples of thresholding techniques applied on an image [14].

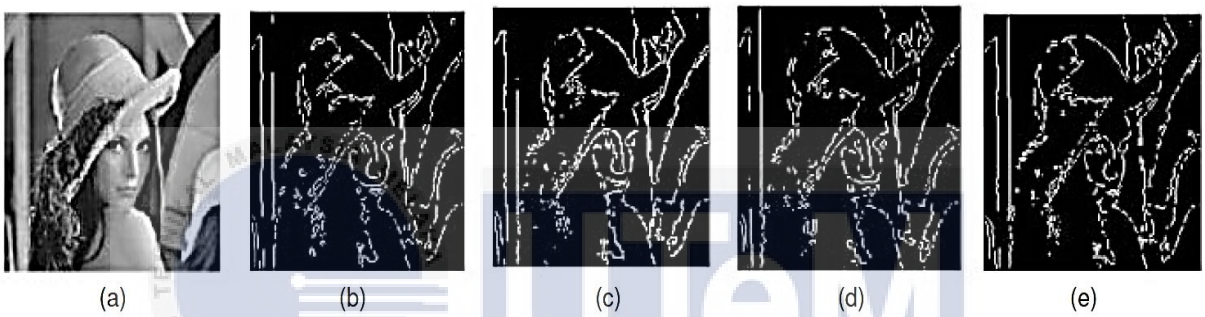

Figure 2.10 Edge detection techniques (a) original image (b) Canny (c) Roberts (d) Sobel (e) Prewitt [14]

UNIVERSITI TEKNIKAL MALAYSIA MELAKA

2.5.2.3 Spatial Based Technique

The spatial based technique are techniques that segments an image into various spatial domain which have similar attributes. Two common spatial based technique are, region growing method; based on its initial pixel and region splitting and merging method; based on adjacent similar region [14].

2.5.2.4 Clustering Technique

The clustering technique are techniques that segments an image into clusters containing similar attribute pixel value. It has two basic specifications in doing the clustering methods which is, hierarchical and partition based. The hierarchical is based on the connection of trees. The highest level of the tree is the whole database on the attributes of the clustered pixel. For the partition based, it uses upgrading methods in

minimizing an objective function. Figure 2.11 shows the example of clustering technique applied on an image [14].

(a) (b)

Figure 2.11 Clustering technique (a) original image (b) clustered image with blue shades [14]

2.5.2.5 Watershed Tecnique

This technique is based on the topological attributes in an image. It represents the intensity of pixels as holes where minima water spills. When the water exceeds the hole, it will merge with other that exceeding its prior hole. This method applies the gradient of the pixel image as a topographic surface. Pixel intensity that have a higher value than the gradient is consider as continuous boundaries Figure 2.12 shows the example of watershed technique applied on an image [14].

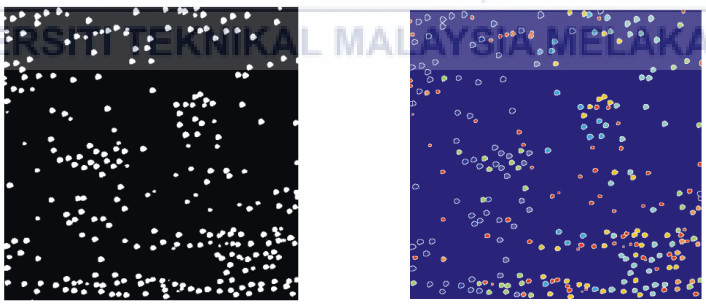

(a) (b)

Figure 2.12 Watershed technique (a) original (b) watershed applied [14]

UNIVERSITI TEKNIKAL MALAYSIA MELAKA

2.5.2.6 PDE Technique

Partial differential equation (PDE) based technique is the fastest technique compared to the other image segmentation technique. The are two fundamental methods in PDE technique which is non-linear isotropic diffusion filter; sharpening edges and convex non-quadratic; remove noise. The outcome from this technique are blurred edges and boundaries [14].

2.5.2.7 ANN Technique

The artificial neural network (ANN) based technique is an independent technique compared to the PDE technique. It uses a big number of linked nodes and in each link has a specific attribute. There two steps in doing this technique which are extracting the image features and segmenting using artificial neural network [14].

2.5.2.8 Summary on Image Segmentation Technique

Table 2.3 shows the summary of image segmentation techniques consist of the thresholding, edge detection, spatial based, clustering based, watershed, PDE and ANN technique [14].

UTeM
اونيۏرسيتي تيکنيکل مليسيا ملاک
UNIVERSITI TEKNIKAL MALAYSIA MELAKA

Table 2.3 Summary on image segmentation techniques [14]

Image Segmentation Technique	**Description**	**Pros**	**Cons**
Thresholding	Depends on the histogram graph of the image in order to find threshold value	Original image information is not needed for further analysis	Highly dependent on histogram analysis peaks and spatial details are not taken into account

Edge detection	Depends on boundary detection in an image	Better distinction between image and unwanted background	Will detect all of the edges including unwanted edges
Spatial Based	Divides pixel of image in from of spatial attributes	Easy to distinguish pixel intensity	Time and storage consumption
Clustering	Divides pixel of image into homogeneous clusters	Usage of fuzzy operator	Complex in determining fuzzy operator parameter
Watershed	Depends on contour region of an image	Consistent in documentation outcome and continuous detection of boundary.	Complexity in gradient evaluation
PDE Based	Applying mathematical concept of differential equations	Low time consumption	Complexity in calculation
ANN Based	Adaptation level simulation of making decision.	Easy to program	Steep learning curve

UNIVERSITI TEKNIKAL MALAYSIA MELAKA

In the recognition and identification of an edge of a butt joint shape, the application of image segmentation, edge detection technique is the optimal solution to be used. Table 2.4 shows the summary of the edge detection techniques in image segmentation [15].

Table 2.4 Summary on edge detection techniques [15]

Operators	**Detection level**	**Operation**	**Advantage**	**Disadvantage**
Sobel	average	Perpendicular angle as the reference in the detection of edge	Simple operation	Unable to obtain accurate outcome on complex images
Prewitt		Horizontal and vertical edges detection.		
Kirsch Edge Detection		Each mask of the method contain edges detected.		
LoG	Mid	Detect doubled edges in an image	Inspects the images in a large scale in the image to find the exact edges in it.	Unable to detect if there is a small amount of edge in an image.
Robert's cross		A two dimensional spatial domain gradient is determined		
Robinson Edge Detection		Each mask of the method contain edges detected.		
Canny Edge Detection	Good	Remove unwanted information such as noise produced and effectively detects edges in an image.	High rate of detection capability, eliminate streaking and adaptive method in various kind of image	Has a high chance to have a false zero crossing.

UNIVERSITI TEKNIKAL MALAYSIA MELAKA

2.5.3 Image Representation and Description

After the image segmentation process, the features of the segmented image can be further represented and described in the image processing. The features of the images are the points of interest which contains distinctive or important information of the image. Table 2.5 shows information of a feature points of an image [24].

Table 2.5 Feature points description [24]

Points	Description
Interest Points	Points in an image that will remain constant despite changes in the pixel's orientation, gradient and scale. Example of interest points are such as corners, edges, blobs and skeleton.
Feature Descriptors	These descriptors describe regional patches in an image around the interest points in vector units. Example of a feature descriptors are raw pixel value, Histogram of gradients and et cetera

2.5.3.1 Skeletonization

Skeletonization is a digital image processing technique that is used to minimize a forepart region in a binary image into a skeletal remainder that highly preserve the topological information of the original regional part while removing most of the forepart pixels. The process of skeletonization makes use of morphological thinning until a medial pixel of one, which continuously erodes the pixel region until no thinning operation is possible resulting in skeleton-like final image. Upon the thinning process, irregularities may occur which will lead to branching in the final image. Pruning can be done to remove these branches to avoid interference in recognition process on the topological information. Figure 2.13 shows the skeletonization process on an image [25].

UNIVERSITI TEKNIKAL MALAYSIA MELAKA

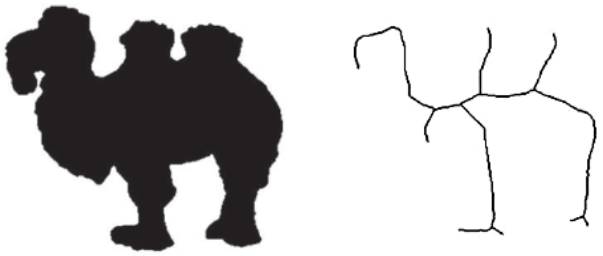

(a) (b)

Figure 2.13 Skeletonization process (a) original (b) skeletonized [25]

2.5.3.2 Corner Detection Techniques

The definition of a corner in a digital image is the postion of a pixel where a small change in the position will cause a huge change in the gradient intensity of a pixel in both x-horizontal and y-vertical axes. Basically, corner detection is the detection of an interest point in the digital image [24]. There are several corner detectors such as, Harris, Shi-Tomasi, Lepetit and Sojka corner detector [22].

- **Harris corner detector**

Harris corner detector detects points of interest by using the Harris operator shown in Equation (2.1) [22].

$$M = G * \begin{pmatrix} I_x^2 & I_x I_y \\ I_x I_y & I_y^2 \end{pmatrix} \quad (2.1)$$

Where G is the size of the Binomial smoothing mask, $I_x I_y$ are the first derivatives of the image gradient that is calculated using the Sobel filter. It determines which region of interest produce a large change in pixel intensity when shifted in both x and y axes directions. Each region of interest is computed with a score R, where a threshold value will be applied to it, to select important corners. Equation (2.2) shows the calculation of the score R.

$$R = \det(M) - k(trace(M))^2 \quad (2.2)$$

Where $\det(M) = \lambda_1 \lambda_2$, λ_1 and λ_2 is the eigenvalues of M, k is an empirical constant between 0.04 to 0.06 and $trace(M) = \lambda_1 + \lambda_2$ [24].

UNIVERSITI TEKNIKAL MALAYSIA MELAKA

- **Shi-Tomasi corner detector**

Shi-Tomasi corner detector computation is similar to that Harris corner detection except for the evaluation of score R. For Shi-Tomasi, the score R is define as the minimum eigenvalues in the pixel, which indicates the most edge of the corners which is represented in Figure 2.14.

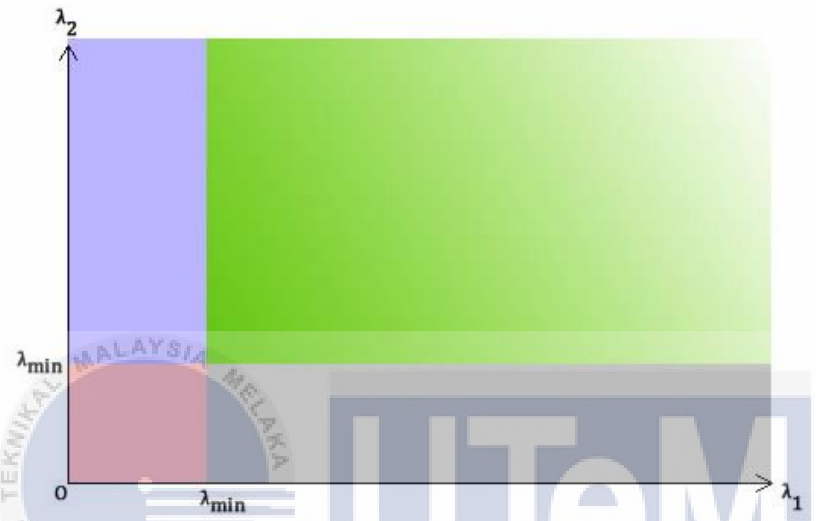

Figure 2.14 Shi-Tomasi corner detection [23]

The green area indicates a corner of a pixel, blue and grey area indicates the edge of the pixel and red indicates the "flat" area. Shi-Tomasi determines the score R as the minimum eigenvalues, λ_{min} in both x and y axes, where it is the most strongest corners [23].

- **Lepetit Points**

Lepetit points determines points of interest such as corners and blobs in an image. The image is then smoothed using a 3 by 3 median filter mask. All the grayscale value intensity is examined. Difference of the grayscale value intensity is computed and a mean value is determined. This method can be used for a high readout speed of point of interest.

UNIVERSITI TEKNIKAL MALAYSIA MELAKA

- **Sojka Points**

Sojka points depicts corner as a point where a two straight and non-collinear grayscale edges intersect. A mask with an adaptive size with its neighboring pixel is applied which will then decide whether a point in an image is a corner. A region of interest is defined that will only be considered in the method. Pixels that has a gradient magnitude less than a minimum intensity are ignored. Only those intersection points are used to form the corner.

2.6 Summary of Related Past Researches

Table 2.6 shows the related research on the recognition and identification of a tooth saw butt joint shape by other researchers. It shows the method done in order to identify the feature points of the edges.

Table 2.6 Related past researches

Author/s Article	**Type of sensor used**	**Type of camera used**	**Shape of the edge of butt joint/weld seam**	**Methodology Description**
H. N. M. Shah, M. Sulaiman, A. Z. Shukor, Z. Kamis, and A. A. Rahman [4]	Vision sensor	CCD camera, 533 × 400 pixel size	Straight, curve and tooth saw shape	Local thresholding of digital image processing technique is used due to variation of lighting condition, shadow and material reflection during recognition of weld seam.
M. Dinham and G. Fang [5]	Vision sensor	CCD stereo camera 1280 ×1024 pixel size	Straight, curve and tooth saw shape	Stereo matching algorithm is used for weld seam identification. Image is captured by two cameras, left and right. The left image is used for extraction of weld seam line and the right image is for

UNIVERSITI TEKNIKAL MALAYSIA MELAKA

				matching feature points calculation.
Y. He, Y. Xu, Y. Chen, H. Chen, and S. Chen [6]	Laser assisted vision sensor	CCD camera, 768 × 576 pixel size	Butt joint	An automatic multi-pass planning using polynomial fitting plus derivatives for feature point extraction of the weld seam profile.
Y. Zou, Y. Wang, W. Zhou, and X. Chen [15]	Laser assisted vision sensor	CMOS camera 1024 × 1280 pixel size	Butt welds, lap welds and curve welds	A target tracking method based on Gaussian kernel was used in extracting the feature points of the weld seam. An adaptive fuzzy controller was designed to input the deviation value of the feature points and the change rate of the deviation into the controller.
Y. Xu et al.[16]	Vision sensor	CCD camera	Straight	A novel software program is used which includes a specific modules, welding power control, intelligent parameter setting, image sensing algorithm, welding database robot communication and path planning modules.
W. J. Shao, Y. Huang, and Y. Zhang [17]	Laser assisted vision sensor	CCD camera 7.4 μm pixel size	V, square, closed square grooves	Used its three laser stripes with different wave length which is projected on the weld seam, two red laser strips are used to measure the three dimensional profile of the weld groove by the principle of optical triangulation, and

UNIVERSITI TEKNIKAL MALAYSIA MELAKA

				the third green laser strip is used as light source to measure the edge and the centerline of the seam by the principle of passive vision sensor.
Y. Zou, X. Chen, G. Gong, and J. Li [18]	Laser assisted vision sensor	CMOS camera 1024 × 1280 pixel size	C, S and butt joint shape	The feature points are obtained using traditional morphological method with aid from the laser assisted vision sensor.
J. Fan, F. Jing, L. Yang, T. Long, and M. Tan [19]	Laser assisted vision sensor	CCD camera 1024 × 1280 pixel size	Straight	A new structured light vision sensor with optical filters and an extra LED light is used to filtered out most of noises from strong arc lights and acquire the image including laser stripe and narrow butt seam. In addition, an image processing method for the vision sensor is designed to obtain feature points butt seams both in horizontal and vertical directions. Two independent Fuzzy-PID controllers are designed to achieve seam tracking control accurately.
J. Zeng, B. Chang, D. Du, Y. Hong, Y. Zou, and S. Chang [20]	Vision sensor and directional lighting manipulation	CCD camera,1600 × 1200 pixel size	Straight	A weld seam recognition method using two directional lights. The directional lights are projected onto the edges of

UNIVERSITI TEKNIKAL MALAYSIA MELAKA

				the seam to produce the distinct man-made “light and shadow” features in order to obtain the edge feature points.
P. Xu, X. Tang, and S. Yao [21]	Laser assisted vision sensor	CCD camera 768×576 pixel size	Curve	A circular laser trajectory used to assist the identification weld seam location and seam tracking.
H. N. Mohd Shah, M. Sulaiman, A. Z. Shukor, M.Z. Ab. Rashid [22]	Vision Sensor	CCD camera, 533 × 400 pixel size	Straight	A CCD is placed as an ideal position to generate information of x and y coordinates. There are four types of corner detection applied, which are Harris binominal, Harris, Lepetit and Sokja points detector.

2.7 Chapter Summary

From the literature review done in this chapter, in order to achieve the objectives of this project, several components and method had been considered and determined to be used in the setup of this project. The objectives of this project is to determine the feature points of the edge of a tooth saw but joint shape using a vision-based approach. Thus, the sensor that will be used is a vision sensor without the assistance of a laser diode. The camera which act as the vision sensor used is the complementary metal-oxide semiconductor (CMOS) camera. The function of the camera is to acquire the original image. The image can be further analyzed using image segmentation, where, in order to detect the edges, the most optimal way is by using edge detection techniques. There are several edge detection techniques that can be applied to achieve the objectives of this project. Therefore, each technique presented in [15] from each sensitivity level will be applied and compared such as, Roberts, Sobel, Prewitt and Canny edge detector. Further process can be done in order to obtain the edges using morphological operation. Dilation is used to enhance the edges

UNIVERSITI TEKNIKAL MALAYSIA MELAKA

detected, further thinning is done to smoothen the edges and skeletonization is used to represent and describe the edges. Finally, in order to identify the feature points of the edges, corner detection technique, Shi-Tomasi will be used to obtain the coordinates of the feature points. Table 2.7 shows the components and methods used in this project and the reasoning behind it.

Table 2.7 Summary of components and methods used

Sensor	• Vision sensor • Simple process, availability and low cost [3]
Camera	• CMOS camera • High readout speed, superior integration and less expensive [10]
Image segmentation technique	• Edge detection technique • Optimal solution for edge of butt joint detection [14]
Edge detection technique	• Canny, Prewitt, Sobel and Roberts • Comparison based on sensitivity level [15]
Morphological image processing	• Dilation, skeletonization and thinning • Optimal solution to represent and decribe the edge of butt joint detected
Corner detection technique	• Shi-Tomasi corner detection technique • High accuracy and easy computation [23]

UNIVERSITI TEKNIKAL MALAYSIA MELAKA

CHAPTER 3

METHODOLOGY

3.1 Overview

In this chapter, the general explanation on the proposed methodology of this project is discussed. The flow of the project is covered. The procedures in validating the reference points, identifying the features points of the edge of the tooth saw butt joint shape using Gradient Based Edge Detection (Roberts, Sobel, Prewitt and Canny) and accuracy & repeatability test are explained

3.2 Project Flowchart

Figure 3.1 shows the flowchart of the project for the identification and recognition of the edge of tooth saw butt joint shape

UTeM
اونيۏرسيتي تيکنيکل مليسيا ملاك
UNIVERSITI TEKNIKAL MALAYSIA MELAKA

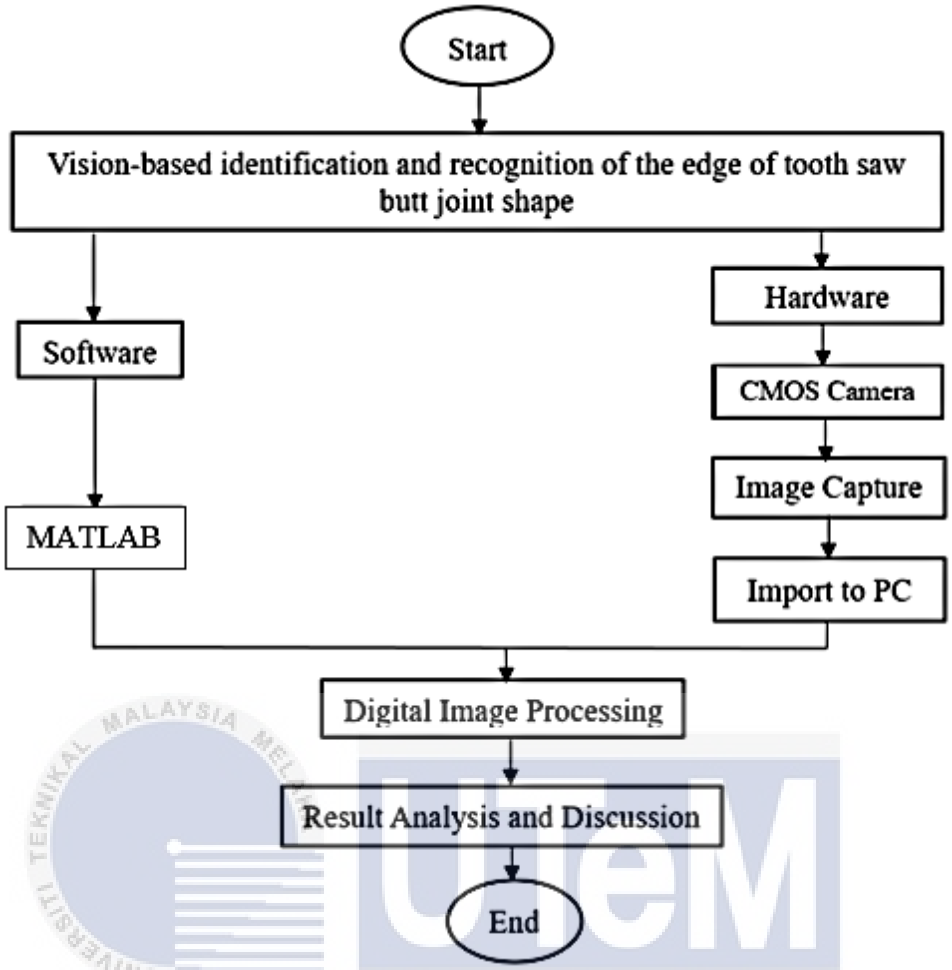

Figure 3.1 Project flowchart

3.3 Experimental Setup

Figure 3.2 shows the experimental setup for this project. CMOS camera with a resolution of 1280x720 pixels size at 30 frames per second is used as the vision sensor to capture the image of the work piece containing the edge of the tooth saw butt joint shape. The camera is placed 20 cm vertically on top of the work piece mounted on a customized stand. A black background work bench is used to make the edge of the tooth saw butt joint shape more visible and ease the process of converting the original image to binary image. The work piece with dimension 100mm × 100mm × 1mm, containing the tooth saw butt joint shape is placed under the camera on top of the workbench in a fixed position to ensure a constant coordinates obtained from the image acquisition by the camera. This project is done in a controlled environment where there is only one light source, which is the external LED light with a variable brightness between 50, 30 and 10 lumens. The LED light is positioned and adjusted until the edge

UNIVERSITI TEKNIKAL MALAYSIA MELAKA

of the tooth saw butt joint shape can be captured clearly by the CMOS camera. The CMOS camera is connected to a PC via micro USB cable to import the image captured. Then, MATLAB Image Processing Toolbox software is used to process the image captured to obtain the feature points of the tooth saw butt joint shape which are the start point, supporting point 1 & 2 and end point in pixel coordinate.

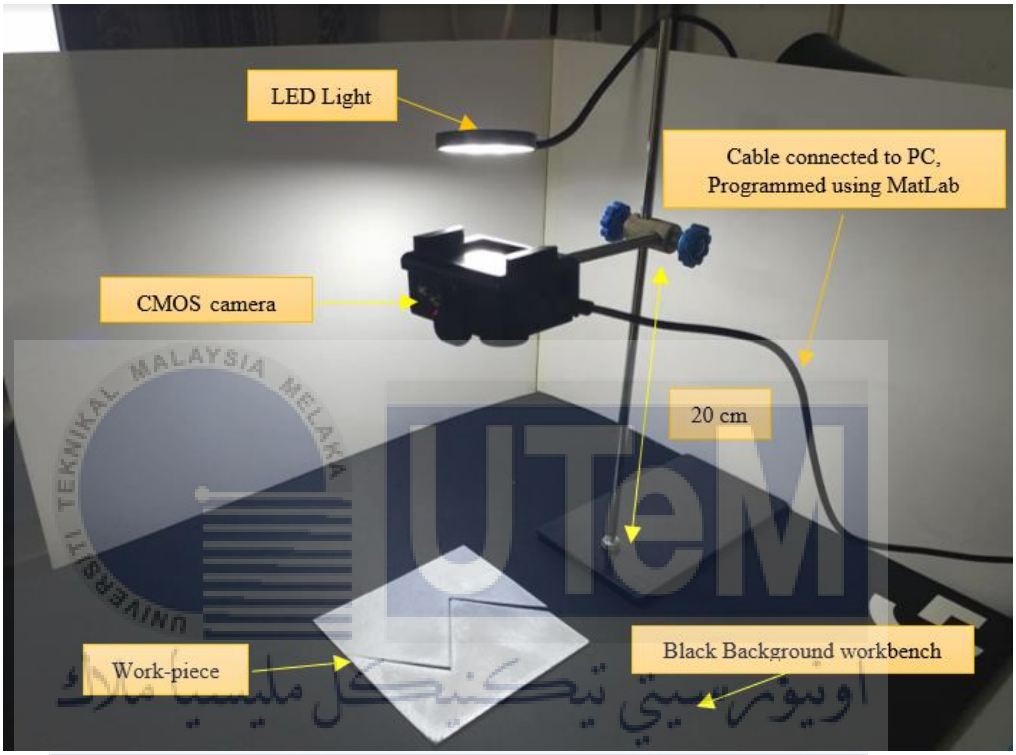

UNIVERSITI TEKNIKAL MALAYSIA MELAKA

Figure 3.2 Experimental setup

In this project, CMOS camera is used for its superior integration system, high readout speed and low cost [9]. An external LED light source is used for its flexibility in design and uniformity of illumination and a hard cardboard that is spray painted with silver color to imitate the reflection behavior of an aluminum sheet is used as the work piece because of its availability. The shape of a tooth saw edge is easily carved out in the middle of the work piece because of its easiness to handle. For the digital image processing, MATLAB software is used because of its numerous amount of matrix library, image processing toolbox and high quality documentation analysis. Table 3.1 show the summary of equipment, parameters and software used in this project.

Table 3.1 Equipment, parameters and software used

Camera	**Type** • Complementary Metal-oxide Semiconductor **Resolution** • 1280x720 @ 30fps **Lens** • 140º wide angle lens **Dimensions** • 60 x 25 x 40 mm **Position** • 20 cm (vertical) mounted on a customized stand **Input / Output** • Micro USB
Illumination	**Type** • 12 circular LEDs **Brightness** • 50, 30 and 10 lumen
Work piece	**Material** • Hard Cardboard **Dimensions** • 100mm × 100mm × 1mm **Color** • Silver **Butt Joint Edge Shape** • Tooth saw
Workbench	**Material** • Synthetic Fabric **Color** • Matte Black
Software	MATLAB Image Processing Toolbox

UNIVERSITI TEKNIKAL MALAYSIA MELAKA

3.4 Preliminary Task: Validation of Reference Points

In order to achieve the first, second and third objectives, this preliminary task is required to be done. The goal of this task is to identify the original feature points of the edge of the tooth saw butt joint shape. The identified points are in pixel coordinates value and denoted as start point, supporting point 1 & 2 and end point. The points act as the reference points for the next experiments. This task also initializes the initial position of the region of interest ROI which will help in the image processing process onwards.

3.4.1 Procedure

Image of the work piece containing the edge of the tooth saw butt joint shape is captured. From the captured image, the start point, supporting point 1 & 2 and end point is marked using human observation and the pixel coordinate for each marked point is recorded. The recorded point is used as the original point of reference for the usage on the next experiments and tasks. The start point is determined as the lowest column of the image and the end point is determined as the highest column of the image. The supporting points are determined from the intersection of the two lines produce by the start and end point with the middle line of the edge tooth saw butt joint. The points for region of interest is also determined. ROI 1 is used as a window which inside the window contains the edge of the tooth saw butt joint shape and ROI 2 is applied for the removal of unwanted edges in the image processing process [4]. Figure 3.3 shows the positions of each feature points that is marked.

UNIVERSITI TEKNIKAL MALAYSIA MELAKA

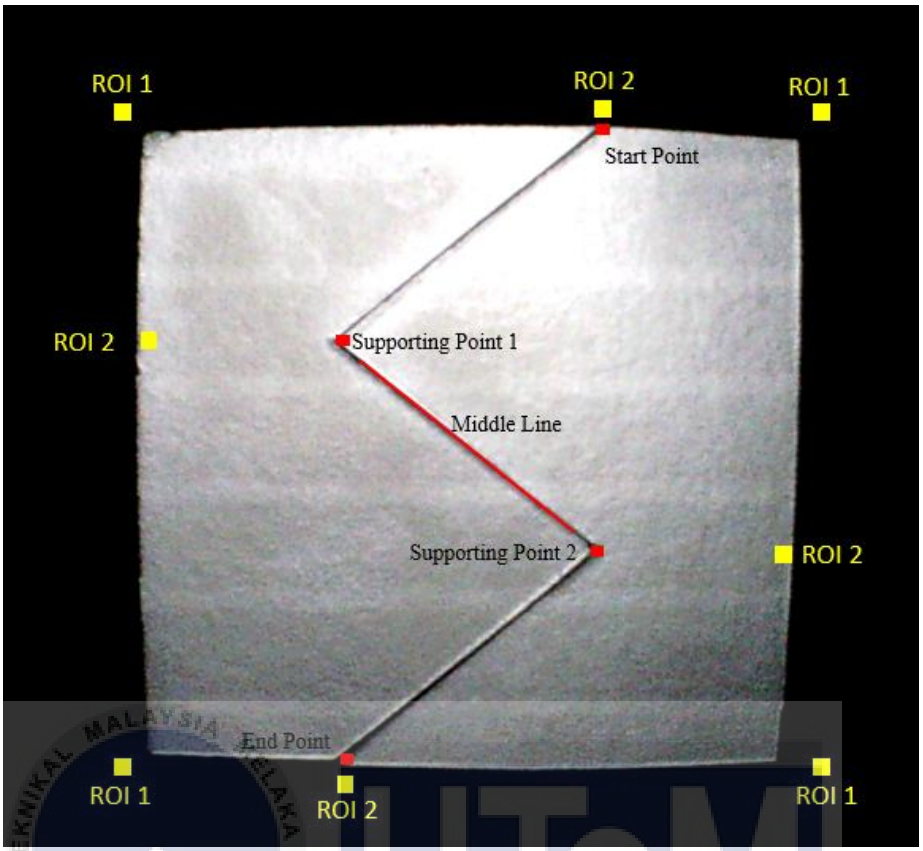

Figure 3.3 Position of marked points

3.5 Experiment 1: Identification of Feature Points of Edge of the Tooth Saw Butt Joint Shape.

For this experiment, it covers on the digital image processing part of the project. It identifies the start point, supporting point 1 & 2 and end point of the edge of the tooth saw butt joint shape using a vision-based system which is by using the CMOS camera, capturing the image of the work piece and MATLAB software to process the image to extract the feature points. The general technique used in the edge detection is by using a gradient based edge detection such as, Canny, Prewitt, Sobel and Roberts edge detector. Figure 3.4 shows the flowchart of this experiment. The results of this experiment covers the first and second objectives.

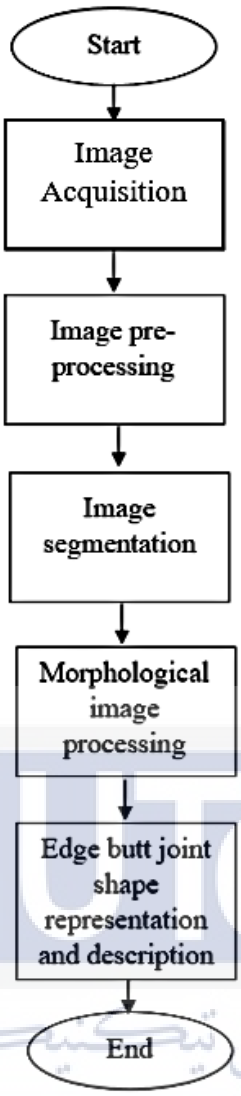

UNIVERSITI TEKNIKAL MALAYSIA MELAKA

Figure 3.4 Experiment 1 flowchart

3.5.1 Procedure

In order to obtain the feature points of the edge of the tooth saw butt joint shape, an analysis on the validation of illumination brightness, threshold values for each edge detection techniques, structuring element size for the morphological operation dilation and corner detection minimum quality is calibrated and determined to find the most optimum value that will give the most precise edge detection reading. Next, the image is acquired and imported to the MATLAB software to undergo the digital image processing which includes the image pre-processing, image segmentation, morphological image processing and the representation and description of the edge of butt joint shape.

3.5.1.1 Validation of Illumination Brightness

This part of the procedure analyzes the most optimal illumination brightness that is used for the image processing step. Illumination plays a big role in image processing process. If the brightness is too high, it will outshine the work piece causing high reflection of light towards the camera causing the edge to be undetected. If it is too low, the camera will not pick up any image, because there is not enough light to reflect the work piece to the lens of the camera [11]. The LED light is a variable light with a brightness of 50, 30 and 10 lumens. Each of the brightness is tested beforehand. The LED is placed on top of the work piece and the image is captured. Then, each of the edge detection technique is tested whether all of them acquire enough information needed to identify the edge of the tooth saw butt joint shape on the binary image. The most optimal brightness will be used on further steps of image processing.

3.5.1.2 Validation of Threshold Value for Edge Detection Techniques

Threshold value in an edge detection technique determines whether a pixel in the image is converted to binary value 1 or 0. In this part of procedure, each of the threshold value is analyzed to find the most optimal value which will give enough information of the edge of tooth saw butt joint shape detected when converted to a binary image. The threshold values will be in between 0 and 1 which correspond to the original images pixel intensity value which is from 0 to 255. For Roberts, Sobel and Prewitt edge detector, there is only one threshold value. If the pixel intensity value is above the threshold, it will be depicted as an edge [23]. The threshold values tested and analyzed are 0.12, 0.14, 0.16 and 0.18. For Canny edge detector, there are two threshold value that is determined whether the pixel intensity value in the original image is an edge, which is a low and high threshold value. If the pixel intensity value is in the range between the two threshold value, it will be defined as an edge [24]. The high threshold value is set to be a constant value of 1 and the low threshold value are tested and analyzed with values 0.2, 0.4, 0.6 and 0.8. Figure 3.5 shows the representation of threshold values of Canny, Prewitt, Sobel and Roberts edge detectors [15].

UNIVERSITI TEKNIKAL MALAYSIA MELAKA

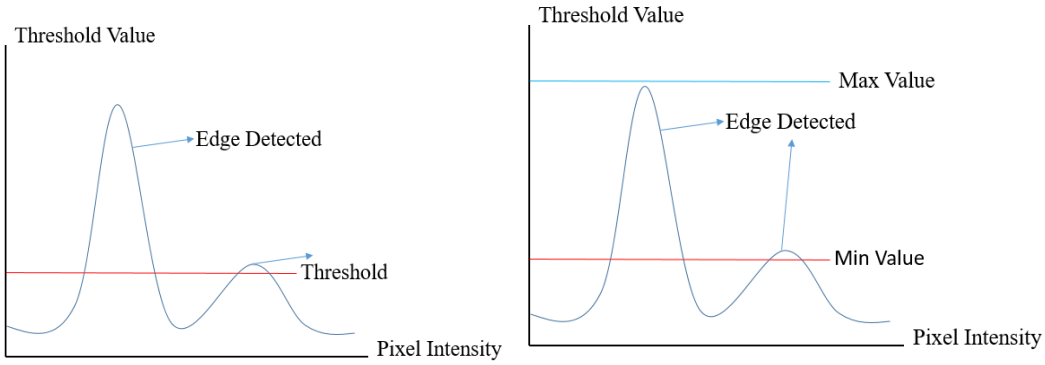

(a) (b)

Figure 3.5 Threshold value (a) Roberts, Sobel and Prewitt (b) Canny edge detector

3.5.1.3 Validation of Structuring Element Size for Morphological Operation Dilation

Morphological operation dilation is part of image processing process to identify the feature points of the edge of the butt joint shape. In this project, the operation combines the double line edges and un-linked edges detected by the edge detection techniques. The intensity of pixel dilated is determined by the size of a structuring element. This analysis determines the optimal size for the structuring element that needed to be used in each of the edge detection techniques. If the size of the structuring element is too large, the intersection line between the start or the end point to the middle will end up combining, thus, when skeletonization process is done, the corner of the supporting point 1 & 2 will be in a curve shape rather than a sharp corner which will affect the coordinates of the feature points. If the size is too small, the un-linked edges will not be combined together, thus, there will be missing edges [13]. Therefore, this analysis determines the optimal size for the structuring element, which in this project, it is the width of the square structuring element with ones matrix. The widths tested are 40, 30, 20 and 10 pixels. Figure 3.6 shows an example of a 10 width pixel of a square structuring element.

UNIVERSITI TEKNIKAL MALAYSIA MELAKA

1	1	1	1	1	1	1	1	1	1
1	1	1	1	1	1	1	1	1	1
1	1	1	1	1	1	1	1	1	1
1	1	1	1	1	1	1	1	1	1
1	1	1	1	1	1	1	1	1	1
1	1	1	1	1	1	1	1	1	1
1	1	1	1	1	1	1	1	1	1
1	1	1	1	1	1	1	1	1	1
1	1	1	1	1	1	1	1	1	1
1	1	1	1	1	1	1	1	1	1

Figure 3.6 10 pixel width square structuring element

3.5.1.4 Validation of Corner Detection Minimum Quality

Shi-Tomasi corner detection method calculates a score which shows the variations of the pixel intensity in both x and y axes. The score is calculated as the minimum eigenvalues of the pixel intensity in both x and y axes. If the score is greater than the threshold determined, it will be defined as a corner. In this procedure, the optimal value for the threshold value which corresponds to the minimum eigenvalues edge detected is analyzed and determined so the feature points of the edge of the tooth saw butt joint shape can be defined accurately. The threshold value that is tested and analyzed are 0.1, 0.2, 0.3 and 0.4. Equation (3.1) shows the corner response to the edge detected based on the threshold values in the image [23].

UNIVERSITI TEKNIKAL MALAYSIA MELAKA

$$R = \begin{cases} \lambda_{min} & if\ \lambda_{min} > T \\ 0 & otherwise \end{cases} \qquad (3.1)$$

where R is the score calculated, λ_{min} is the minimum eigenvalues and T is the threshold value determined.

3.5.1.5 Image Pre-Processing

In this procedure, by using MatLab, a window or a region of interest (ROI) is created which encloses the portion of the captured image containing enough information on the edge of the tooth saw butt joint shape for further operation. The window is in rectangular shape using the function "roipoly(img,r,c)" where "img" is

the original image capture, “r” is the row coordinates and “c” is the column coordinates of the original image. These coordinates had been pre-determined on the first preliminary task, which is the coordinates of ROI 1. The region of interest creates a mask with binary values. This binary mask for the image sets pixels inside the region of interest as 1 and pixels outside the region of interest as 0. The region of interest which had been depicted as 1 is then converted back to the original image section. Thus, by doing so, it filters and isolates the image containing the edge of the tooth saw butt joint shape from unnecessary background [4].

3.5.1.6 Image Segmentation

In this procedure, edge detection method is used in order to detect the edge of the tooth saw butt joint shape. The edge detection method that is used is the gradient based edge detection which is by using Roberts, Sobel, Prewitt and Canny Operator. The original image captured is a function of two variables, $img(i,j)$ where img is the function of the original image which returns the intensity pixel value of the original image at point (i,j). The point (i,j) is the intensity value of each pixel in the original image, which is between 0 to 255. Thus, the derivative for the function $img(i,j)$ is depicted as Equation (3.2) [15].

$$\nabla img = i\frac{\partial img(i,j)}{\partial i} + j\frac{\partial img(i,j)}{\partial j} \tag{3.2}$$

where $i\frac{\partial img(i,j)}{\partial i}$ is the gradient for horizontal direction and $j\frac{\partial img(i,j)}{\partial j}$ is the gradient for vertical direction. The gradient magnitude, $|G|$ of the original image can be depicted as Equation (3.3) [15].

$$|G| = \sqrt{\left(\frac{\partial img(i,j)}{\partial i}\right)^2 + \left(\frac{\partial img(i,j)}{\partial j}\right)^2} \tag{3.3}$$

UNIVERSITI TEKNIKAL MALAYSIA MELAKA

- **Roberts, Sobel and Prewitt Edge Detection**

Roberts operators calculates the two dimensional spatial gradient on the original image. It highlights the parts of the original image with high spatial gradient which indicates that it is an edge. The spatial gradient is calculated by convoluting the original image using a 2x2 matrices. Sobel operator calculates the approximation gradient of the pixel image intensity function of the edge detection. It uses a 3 x 3 kernels to detect the edges vertically and horizontally relative to the original image pixel grid. Prewitt operator detects edges same as Sobel operator but with different kernel mask and does better detection than Sobel operator. There are 5 steps in the algorithm of the 3 gradient based edge detection that are done in the MATLAB software which are:

Step 1: The original image is pre-processed using filters in order to reduce noise.

Step 2: The original image is convoluted in the horizontal direction using the x-kernel gradient component, D_x of each gradient based edge detection operation, where Equation (3.4) is for Roberts (3.5) for Sobel and (3.6) for Prewitt operator [15].

$$D_x = \begin{bmatrix} 1 & 0 \\ 0 & -1 \end{bmatrix} \tag{3.4}$$

UNIVERSITI TEKNIKAL MALAYSIA MELAKA

$$D_x = \begin{bmatrix} -1 & 0 & +1 \\ -2 & 0 & +2 \\ -1 & 0 & +1 \end{bmatrix} \tag{3.5}$$

$$D_x = \begin{bmatrix} -1 & 0 & +1 \\ -1 & 0 & +1 \\ -1 & 0 & +1 \end{bmatrix} \tag{3.6}$$

Step 3: The original image is convoluted in the vertical direction using the y-kernel gradient component, D_y of each gradient based edge detection operation, where Equation (3.7) is for Roberts (3.8) for Sobel and (3.9) for Prewitt operator [15].

$$D_y = \begin{bmatrix} 0 & 1 \\ -1 & 0 \end{bmatrix} \tag{3.7}$$

$$D_y = \begin{bmatrix} -1 & 0 & +1 \\ -2 & 0 & +2 \\ -1 & 0 & +1 \end{bmatrix} \quad (3.8)$$

$$D_y = \begin{bmatrix} +1 & +1 & +1 \\ 0 & 0 & 0 \\ -1 & -1 & -1 \end{bmatrix} \quad (3.9)$$

Step 4: The magnitude of the gradient components for each pixel in the original image is calculated using Equation (3.10) and compared with a threshold that had been chosen from the validation of threshold value analysis. If the magnitude value calculated is greater than the threshold value, the pixel will be defined as an edge and converted as a binary image with value of 1. If the magnitude value calculated is lower than the threshold value, the pixel will be defined as unnecessary pixel and converted as a binary image with value of 0 [24].

$$|D| = \sqrt{D_x^2 + D_y^2} \quad (3.10)$$

Step 5: The steps from 1 to 4 is repeated for each of the pixel in the original image.

- **Canny Edge Detection**

For the Canny edge detection technique, it has extra steps in defining an edge and uses the output of the Sobel operator. The algorithm isolates the background noise from the image to find discontinuities boundary which is the edge of the tooth saw butt joint shape in the image captured. Canny edge detection provides the most optimal solution to remove noise from image due to these extra steps [15]. There are 6 steps in the algorithm of the Canny edge detection method done in the MATLAB software which are:

Step 1: Gaussian filter is used to smoothen the image inside the region of interest, removing noise and unwanted information using Equation (3.11) and (3.12) [24].

$$g(x, y) = G\sigma(i, j) * img(i, j) \quad (3.11)$$

UNIVERSITI TEKNIKAL MALAYSIA MELAKA

$$G\sigma = \frac{1}{\sqrt{2\pi\sigma^2}} e^{\left(-\frac{i^2+j^2}{2\sigma^2}\right)} \tag{3.12}$$

where $G\sigma(i,j)$, is the Gaussian filter, $img(i,j)$ is the original image captured, $g(x,y)$ is the smoothed image and σ is the standard deviation referring to the Gaussian filter.

Step 2: The edges from the original image captured is calculated by applying the gradient to x and y coordinates of the captured image using Equation (3.13) [24].

$$M(x,y) = \sqrt{g_x^2(x,y) + g_y^2(x,y)} \tag{3.13}$$

where $M(x,y)$ is the gradient, $g_x(x,y)$ and $g_y(x,y)$ are x and y coordinates respectively.

Step 3: The edges of the captured image is traced by defining a threshold using the x and y coordinates using Equation (3.14) [24].

$$M_T(x,y)\begin{cases} M(x,y) \; if \; M(x,y) > T \\ 0 \qquad\qquad otherwise \end{cases} \tag{3.14}$$

where $M_T(x,y)$ is the threshold value determined from the analysis of the validation of threshold value. The threshold value will determine where it will keep the information of the edge of the tooth saw butt joint shape and remove most of the noise present.

Step 4: The non-maximum pixels of the edge of the tooth saw butt joint shape is suppressed to obtain from the threshold M_T . To suppress it, each of the non-zero threshold determines whether it is greater than its neighboring pixels along the gradient. If it is greater, the threshold will not change. If it is less, it is set to 0.

Step 5: In this step, the result from step 4 will be threshold to obtain two other different threshold which will be set as $\tau_1$and τ_2 which τ_1 is defined as the high level and τ_2 is defined as the low level. By doing so, two binary image will be generated and defined as $T_1$and T_2.

Step 6: The final step is to link the edges in T_2. To do this, each pixel that is defined as the edge in T_2 will be located and the edge segmented of its neighbor binary image T_1 will also be located to link between both of the binary image. Thus a continuous edge will be formed.

3.5.1.7 Morphological Image Processing

From the previous step, there is a double edges in parallel that forms the tooth saw butt joint shape or un-linked edges. In this procedure dilation is performed to combined those double and un-linked edges to form a single edge. The double and un-linked edges are combined and dilated using a square structuring element with a pre-determined width that is obtained from the analysis for the validation of the structuring element size. Equation (3.15) [13] shows the overview process of the dilation process that is done in the MATLAB software.

$$A \oplus B = \{s\mathrm{I}(\hat{B})s \cap A\} \tag{3.15}$$

where A is the segmented binary image using edge detection technique, B is the square structuring element, $\hat{B}$ is the reflection of B about its origin which is followed by a shift of s [13].

UNIVERSITI TEKNIKAL MALAYSIA MELAKA

3.5.1.8 Edge Butt Joint Shape Representation and Description

This is the final procedure in order to obtain the feature points of the edge of the tooth saw butt joint shape. Skeletonization technique in the MATLAB software is used onto the binary image after the morphological operation dilation step. This results in all the object inside the image converted to lines by thinning process, where it peels the contour of the edge of the tooth saw butt joint shape detected until it reaches most medial one-pixel width whilst preserving the topology of the edge shape [24]. Thus, the edge of tooth saw butt joint shape on the image is converted to a single line, which enables for the features points of the edge to be determined. The feature points are obtained by using Shi-Tomasi corner detection method. The method calculates a score which shows the variations of the pixel intensity in both x and y axes. The score is

calculated as the minimum eigenvalues of the pixel intensity in both x and y axes. Then a threshold is determined from the analysis of validation of minimum quality for corner detection. If the score is greater than the threshold determined, it will be defined as a corner. Equation (3.16) shows the overview formula for the Shi-Tomasi corner detection method [23].

$$R = min(\lambda_1, \lambda_2) \tag{3.16}$$

where R is the score and λ_1 and λ_2 is the eigenvalues of the pixel intensity in both x and y axes.

3.6 Experiment 2: Accuracy Test

For this experiment, the identification of feature points of edge of the tooth saw butt joint shape using gradient based edge detection (Canny, Prewitt, Sobel & Roberts) is repeated for 10 times using the determined variables, which is the threshold value, structuring element size for the morphological operation dilation and the corner detection minimum quality. Each of the average result by using Equation (3.17) of the repeated experiment is recorded.

اونيۏرسيتي تيكنيكل مليسيا ملاك
UNIVERSITI TEKNIKAL MALAYSIA MELAKA

$$\bar{x} = \frac{\sum x_n}{n} \tag{3.17}$$

where $\bar{x}$, is the average reading, $\sum x_n$ is the summation of each reading of the feature points detected and n is the number of reading obtained.

The average coordinates of the feature points identified using each of the edge detection techniques are compared with the original point obtained from the validation of reference point. The accuracy is analyzed by determining which method identifies its features points near to the original refernce point using Equation (3.18).

Δ(x,y) = Original Point (x, y pixel) - Identified Point (x, y pixel) (Mean, $\bar{x}$) (3.18)

3.7 Experiment 3: Repeatability Test

This experiment determines whether each of the edge detection technique able to produce reliable results by repeating each of the techniques using the same procedures and same variables. The average reading from the previous experiment is used to calculated the standard deviation. Low standard deviation value indicates that the method has less variation in the readings, thus high repeatability and reliability of the methods, procedures and variables used. Equation (3.19) shows the formula to calculate standard deviation

$$s = \sqrt{\frac{\sum(x_n - \bar{x})^2}{n-1}} \tag{3.19}$$

where x_n is the value of each reading, $\bar{x}$ is the average reading and n is the number of reading obtained.

3.8 Chapter Summary

In this project, there are one preliminary task and three experiment in order to achieve the objectives of the project. The task mentioned is to validate the original point of the edge of tooth saw butt joint shape feature using human observation. The first experiment is to identify the start point, supporting points and end point of the tooth saw butt joint shape using gradient based edge detection (Canny, Prewitt, Sobel & Roberts) techniques in MATLAB software. The next experiment is to test the accuracy by comparing the identified points from the first experiment for each gradient based edge detection technique used with the original point obtained from the preliminary task. The last experiment is to evaluate the repeatability of the techniques used in identifying the start point, supporting points and end point of a tooth saw butt joint shape. Table 3.2 shows the summarization of the task and experiments required to be done to achieve the objectives of the project.

UNIVERSITI TEKNIKAL MALAYSIA MELAKA

Table 3.2 Summarization of task and experiments

	Objective 1	Objective 2	Objective 3	Objective 4
Preliminary Task	√	√	√	√
Experiment 1	√	√		
Experiment 2			√	
Experiment 3				√

For the preliminary task, the reference points are determined using human observation. There will be some systematic errors in defining the original feature points. These identified original points will only be a reference to the points identified by the computer using digital image processing. The comparison between the identified original points and the identified points using the digital image processing will highlight the range of errors occurred in terms of the coordinate x and y pixel value. But it is estimated that the errors will be minimal due to the detailed observation done. For the first experiment, it is expected to have some random errors in recognizing and identifying the edges and its feature points. This is because each of the edge detection techniques has a chance to have a false zero crossing, meaning that unwanted edges will also be detected. Those errors will affect the corners detected, thus having a different coordinate from the original points. Therefore, in between the image processing, the validation of illumination brightness, threshold value for the edge detectors, structuring element size for dilation operation and minimum quality for corner detector are analyzed thoroughly. A range of value is analyzed for all the variables mentioned. This will help in the accuracy of the methods to define the feature points of the edge of the tooth saw butt joint shape. The operation is repeated for ten times to reduce the random errors, which is an error that occurs due to variations of readings. The operation will also might be repeated for more than ten times due to errors in the software itself. From the repeated operation, the average readings are used for the evaluation of experiment 2 and 3 to reduce the errors of miscalculations. Thus, the objectives of this project can be achieved with reduced errors.

UNIVERSITI TEKNIKAL MALAYSIA MELAKA

CHAPTER 4

RESULT AND DISCUSSION

4.1 Overview

In this chapter, the results for the proposed edge detection methods in Chapter 3 is presented and explained. The results for the preliminary task, experiment 1, experiment 2 and experiment 3 is in the form of figures and tables. The analysis on the accuracy and repeatability on the proposed methods is discussed.

4.2 Preliminary Task: Validation of Reference Points

Figure 4.1 shows the original image captured containing the edge of tooth saw butt joint shape. Each of the features point such as the starting point, supporting point 1 & 2 and end point is chosen and marked using human observation. Other important constant pixel points are also marked such as the ROI 1 and ROI 2 for the usage of image processing process.

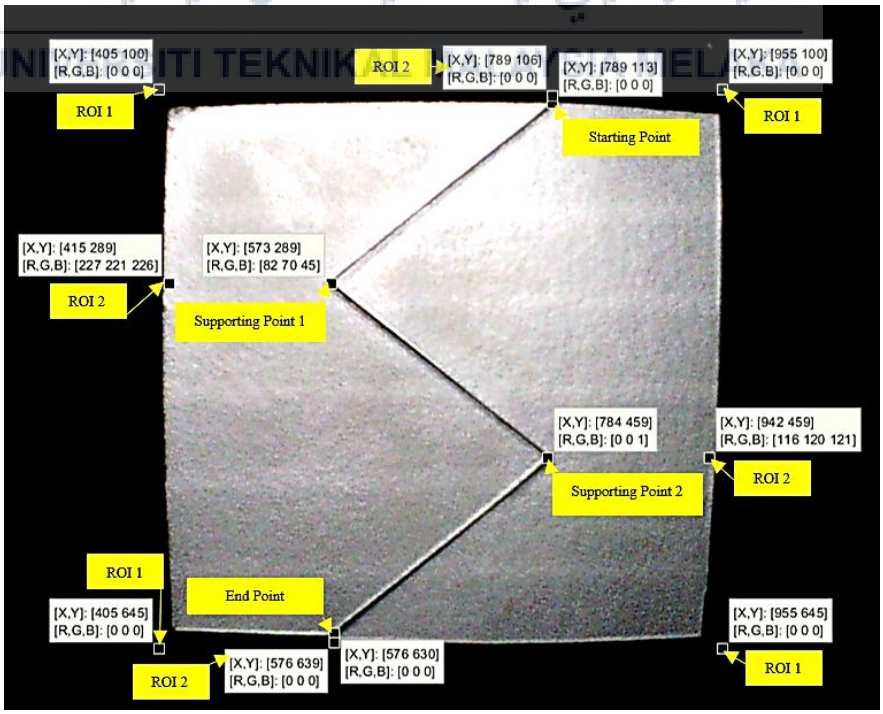

Figure 4.1 Marked Points

Table 4.1 and 4.2 shows the results for the preliminary task. The original start point, supporting point 1 & 2 and end point of the edge of the tooth saw butt joint shape obtained are in x and y coordinate pixel value. These points will act as the reference point for the following experiment.

Table 4.1 Original points

Point	Original Point (x, y pixel)
Start	789, 113
Supporting 1	574, 289
Supporting 2	784, 459
End	576, 630

Table 4.2 ROI points

Point	ROI 1 (x, y pixel)	ROI 2 (x, y pixel)
1	405, 100	789, 106
2	955, 100	942, 459
3	955, 645	576, 639
4	405, 645	415, 289

4.3 Experiment 1: Identification of Feature Points of Edge of the Tooth Saw Butt Joint Shape.

This part contains the results of the validation of illumination brightness, threshold value for edge detection techniques, structuring element size for the morphological operation dilation, corner detection minimum quality and identified feature points of the edge of the tooth saw butt joint shape.

4.3.1 Validation of Illumination Brightness

Figure 4.2 shows the results on the effects of different illumination brightness towards each edge detection techniques.

UNIVERSITI TEKNIKAL MALAYSIA MELAKA

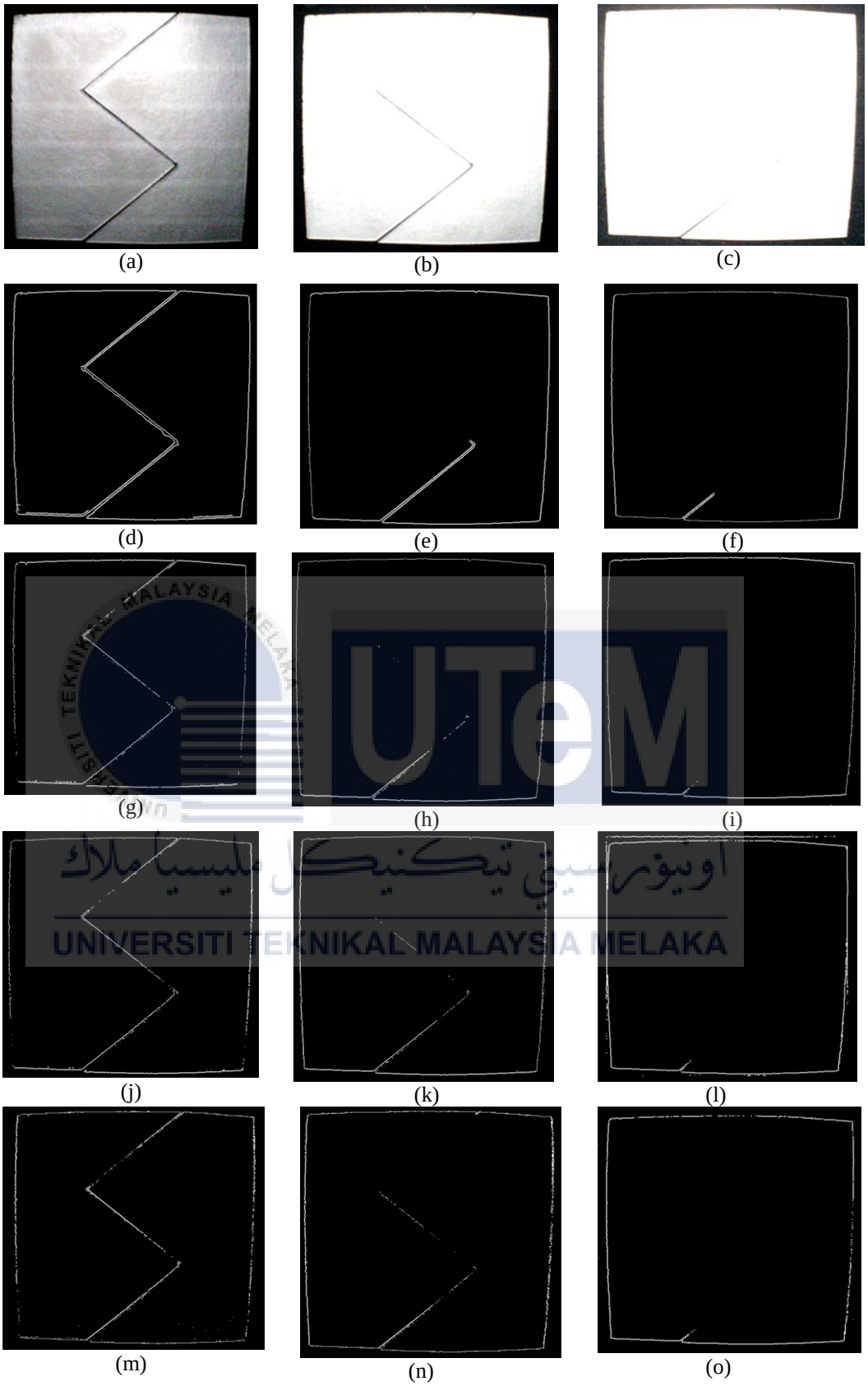

Figure 4.2 Brightness (a) 10 (b) 30 (c) 50 lumens effects on (d-f) Canny (g-i) Prewitt (j-l) Sobel and (m-o) Roberts edge detection techniques

UNIVERSITI TEKNIKAL MALAYSIA MELAKA

From the observation of Figure 4.2, the LED, with brightness 10 lumens has the highest image quality and each of the edge detector, Canny, Prewitt, Sobel and Roberts can detect enough information of the edge of the tooth saw butt joint shape. LED with brightness 30 and 50 lumen exhibit a poor quality of image due to the over exposure from the reflection of light [11] from the surface of the work piece to the camera lens and each of the edge detector did not detect enough information on the edge of the tooth saw butt joint shape thus resulting in edge loss. Therefore, Illumination brightness of 10 lumens is the most optimal value to be used for the image processing process.

4.3.2 Validation of Threshold Value for Edge Detection Techniques

This first part of this analysis shows the effects of threshold values of edge detection for Roberts, Sobel and Prewitt edge detector with values 0.12, 0.14, 0.16 and 0.18. The second part shows the threshold values of edge detection for Canny edge detector with value 0.2, 0.4, 0.6 and 0.8.

4.3.2.1 Roberts, Sobel and Prewitt Edge Detection

Figure 4.3 shows the effect of threshold value 0.12 towards each detection techniques, Roberts, Sobel and Prewitt edge detector.

UNIVERSITI TEKNIKAL MALAYSIA MELAKA

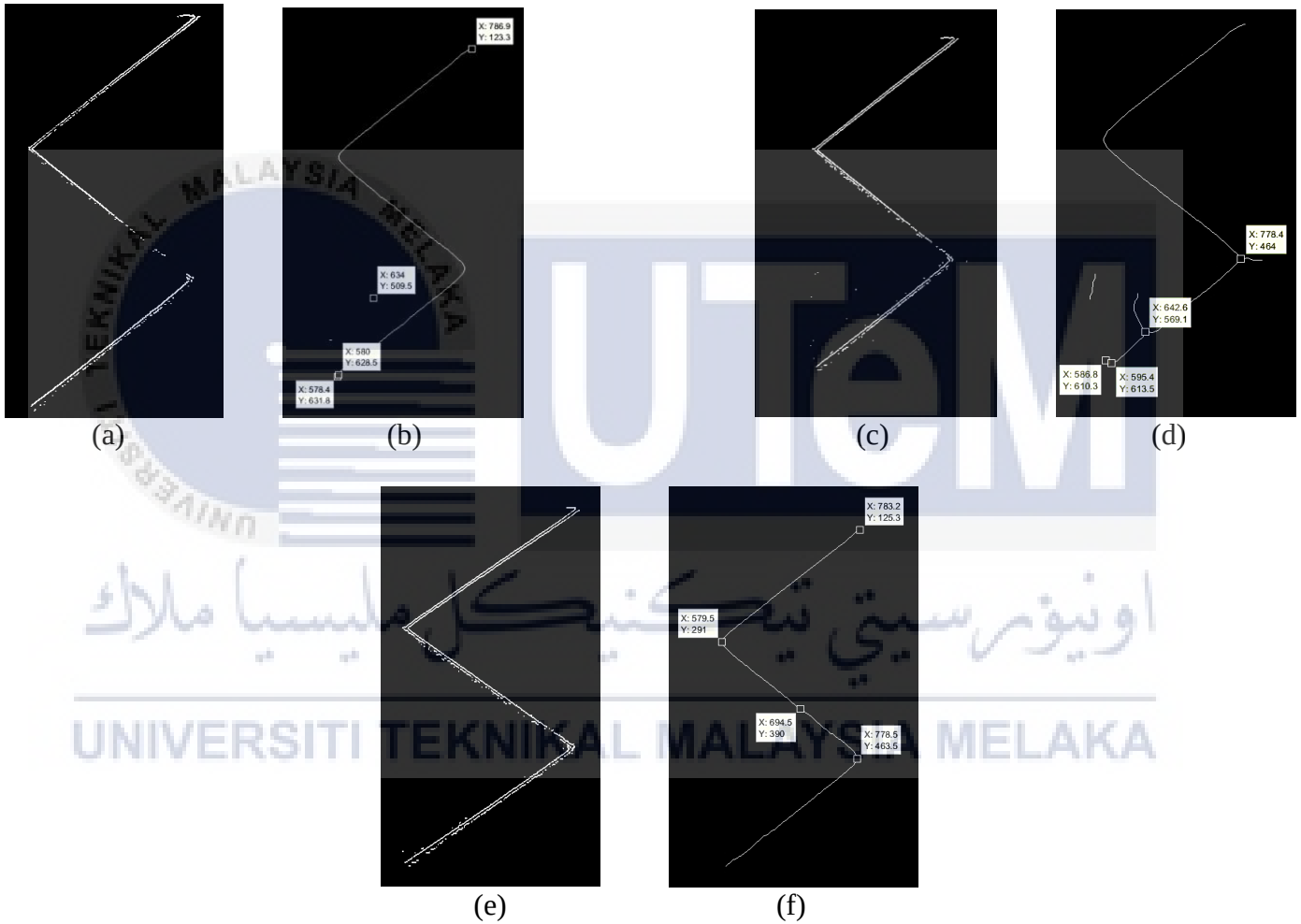

(a) (b) (c) (d)

(e) (f)

Figure 4.3 Threshold value of 0.12 effects on (a-b) Roberts, (c-d) Sobel and (e-f) Prewitt edge detection

UNIVERSITI TEKNIKAL MALAYSIA MELAKA
اونيۏرسيتي تيکنيکل مليسيا ملاک

Based on Figure 4.3, it shows that each of the edge detection techniques detects enough information on the edge of the tooth saw butt joint shape but, there is a small amount of unwanted edges that were detected as well. This is because the threshold value of 0.12 is too low causing some of the pixel intensity of the unwanted edges to surpass the threshold value, thus it is taken into account as an important edges. Therefore, after image processing, there are too many corners detected in the final image causing a large error in the pixel coordinates compared to the original points. Table 4.3 shows the pixel coordinates and errors of each edge detection techniques with threshold value of 0.12.

Table 4.3 Edge detection with threshold value 0.12

Point	**Original Point (x, y pixel)**	**Identified Point (x, y pixel)**	**Error (Δx, Δy)**
Roberts edge detection with threshold 0.12			
Start	789.0, 113.0	786.9, 123.3	2.1, -10.3
Supporting 1	574.0, 289.0	634.0, 509.5	-60, -220.5
Supporting 2	784.0, 459.0	580.0, 628.5	204, 169.5
End	576.0, 630.0	578.4, 631.8	-2.4, -1.8
Sobel edge detection with threshold 0.12			
Start	789.0, 113.0	778.4, 464.0	10.6, -351.0
Supporting 1	574.0, 289.0	642.6, 569.1	-68.6, -280.1
Supporting 2	784.0, 459.0	586.8, 610.3	197.2, -151.3
End	576.0, 630.0	595.4, 613.5	-19.4, 16.5
Prewitt edge detection with threshold 0.12			
Start	789.0, 113.0	783.2, 125.3	5.8, -12.3
Supporting 1	574.0, 289.0	579.5, 291.0	-5.5, -2.0
Supporting 2	784.0, 459.0	694.5, 390.0	89.5, 69.0
End	576.0, 630.0	778.5, 463.5	-202.5, 166.5

Figure 4.4 shows the effect of threshold value 0.14 towards each detection techniques, Roberts, Sobel and Prewitt edge detector.

UNIVERSITI TEKNIKAL MALAYSIA MELAKA

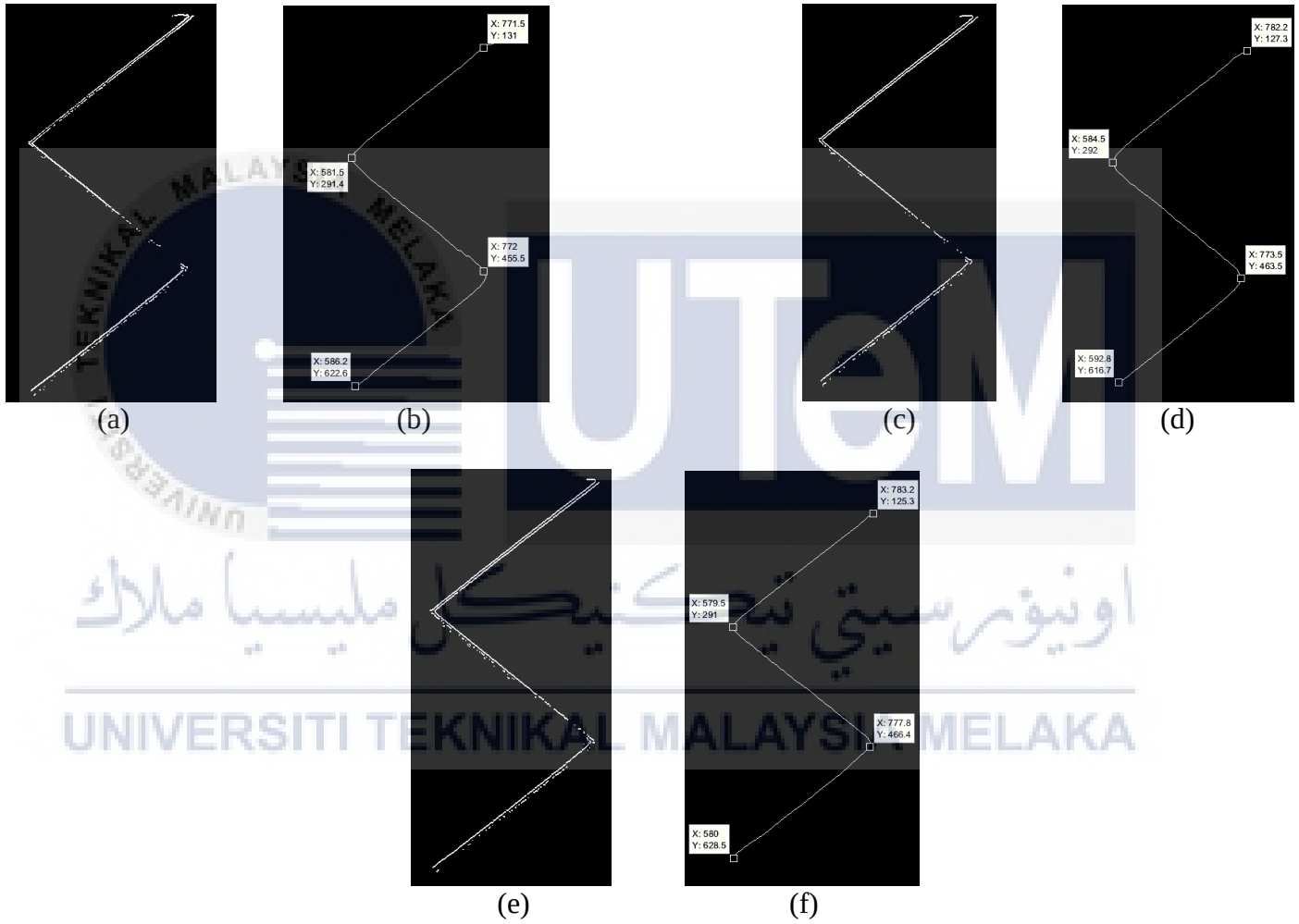

(a) (b) (c) (d)

(e) (f)

Figure 4.4 Threshold value of 0.14 effects on (a-b) Roberts, (c-d) Sobel and (e-f) Prewitt edge detection

UNIVERSITI TEKNIKAL MALAYSIA MELAKA

Based on Figure 4.4, it shows that there is a perfect amount of information of the edge of tooth saw butt joint shape detected by each of the edge detection techniques. All the unwanted small edges had been successfully thresholded. This shows that the threshold value of 0.14 is an optimal value, where the intensity pixel value of the unwanted edges are not high enough to surpass the threshold value causing it to be defined as not an important edge. Therefore, after image processing process, the corner detector can easily detect the feature points of the edges of the tooth saw butt joint shape with a close value of coordinates with the original edges. Table 4.4 shows the pixel coordinates and errors of each edge detection techniques with threshold value of 0.14.

Table 4.4 Edge detection with threshold value 0.14

Point	**Original Point (x, y pixel)**	**Identified Point (x, y pixel)**	**Error (Δx, Δy)**
Roberts edge detection with threshold value 0.14			
Start	789.0, 113.0	771.5, 131.0	17.5, -18
Supporting 1	574.0, 289.0	581.5, 291.4	-7.5, -2.4
Supporting 2	784.0, 459.0	772.0 455.5	12, 3.5
End	576.0, 630.0	586.2, 622.6	-10.2, 7.4
Sobel edge detection with threshold value 0.14			
Start	789.0, 113.0	782.2, 127.3	6.8, -14.3
Supporting 1	574.0, 289.0	584.5, 292.0	-10.5, -3.0
Supporting 2	784.0, 459.0	773.5, 463.5	11.0, -4.5
End	576.0, 630.0	592.8, 616.7	-16.8, 13.3
Prewitt edge detection with threshold value 0.14			
Start	789.0, 113.0	782.2, 127.3	6.8, -14.3
Supporting 1	574.0, 289.0	584.5, 292.0	-10.5, -3.0
Supporting 2	784.0, 459.0	773.5, 463.5	11.0, -4.5
End	576.0, 630.0	592.8, 616.7	-16.8, 13.3

Figure 4.5 shows the effect of threshold value 0.16 towards each detection techniques Roberts, Sobel and Prewitt edge detector.

UNIVERSITI TEKNIKAL MALAYSIA MELAKA

Figure 4.5 Threshold value of 0.16 effects on (a-b) Roberts, (c-d) Sobel and (e-f) Prewitt edge detection

UNIVERSITI TEKNIKAL MALAYSIA MELAKA

From Figure 4.5, it can be observed that Roberts edge detector has removed some of the important edges, resulting in un-linked edges. This shows that threshold value of 0.16 is too high for Roberts as the important edges pixel intensity does not surpass the threshold value. Although Sobel and Prewitt edge detector detects enough information on the important edges, there is still some of the important edges being removed resulting in losing its topological characteristic causing error in the feature points coordinate reading. Table 4.5 shows the pixel coordinates and errors of each edge detection techniques with threshold value of 0.16.

Table 4.5 Edge detection with threshold value 0.16

Point	**Original Point (x, y pixel)**	**Identified Point (x, y pixel)**	**Error (Δx, Δy)**
Roberts edge detection with threshold value 0.16			
Start	789.0, 113.0	583.0, 287.5	206.0, -174.5
Supporting 1	574.0, 289.0	581.5, 291.5	-7.5, -2.5
Supporting 2	784.0, 459.0	692.8, 386.6	91.2, 102.4
End	576.0, 630.0	582.2, 622.6	-6.2, 7.4
Sobel edge detection with threshold value 0.16			
Start	789.0, 113.0	783.5, 126.3	5.5, 13.3
Supporting 1	574.0, 289.0	585.5, 290.0	-11.5, -1.0
Supporting 2	784.0, 459.0	771.0, 463.0	13, -4.0
End	576.0, 630.0	587.2, 619.6	-11.2, 10.4
Prewitt edge detection with threshold value 0.16			
Start	789.0, 113.0	783.2, 125.3	5.8, 12.3
Supporting 1	574.0, 289.0	579.5, 291.0	-5.5, -2.0
Supporting 2	784.0, 459.0	779.5, 461.5	6.2, -2.5
End	576.0, 630.0	581,0, 627.5	-5.0, -2.5

Figure 4.6 shows the effect of threshold value 0.18 towards each detection techniques Roberts, Sobel and Prewitt.

UNIVERSITI TEKNIKAL MALAYSIA MELAKA

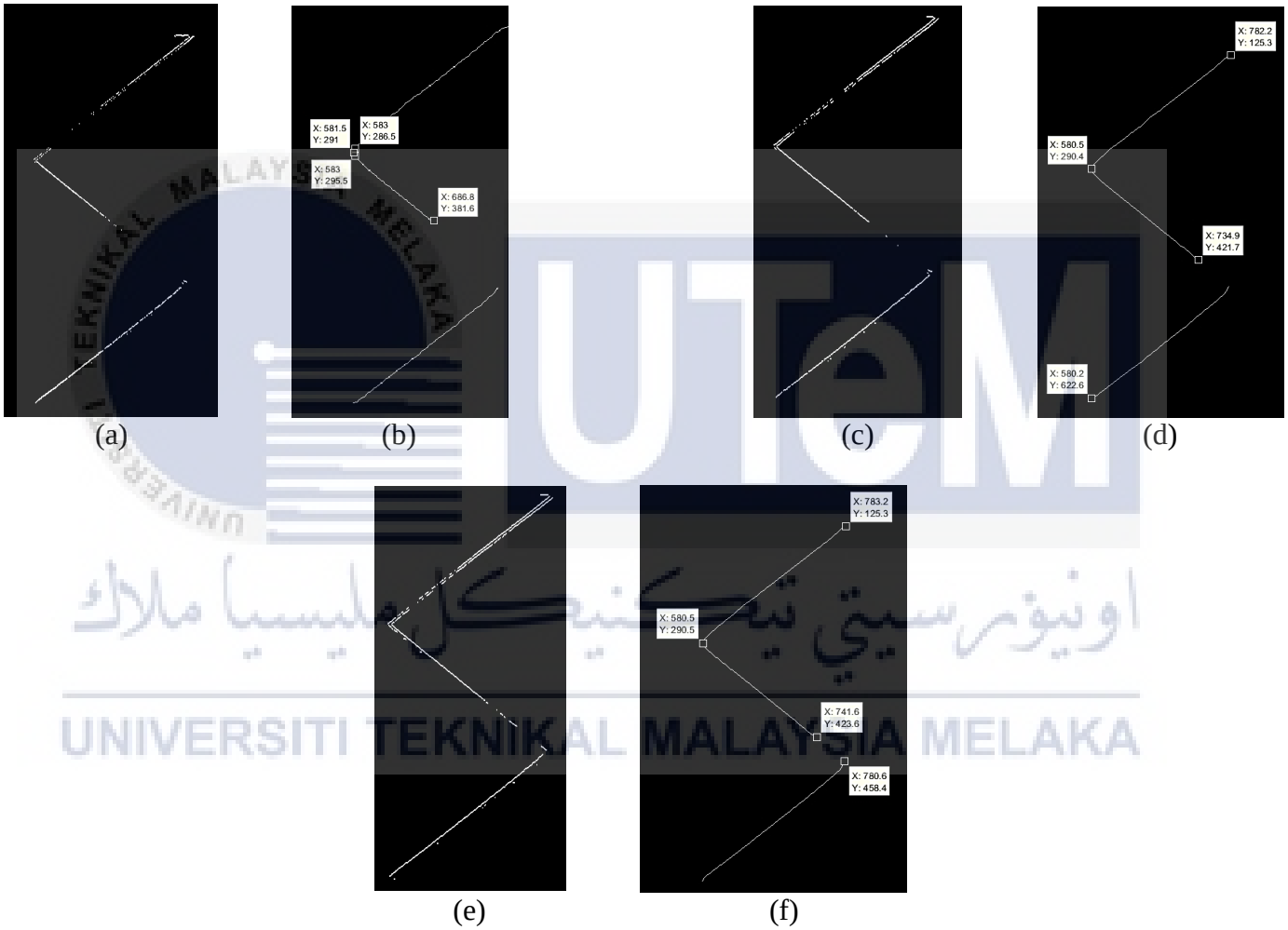

(a) (b) (c) (d)

(e) (f)

Figure 4.6 Threshold value of 0.18 effects on (a-b) Roberts, (c-d) Sobel and (e-f) Prewitt edge detection

UNIVERSITI TEKNIKAL MALAYSIA MELAKA

From Figure 4.6, it is observed that there is not enough amount of information on the important edges detected because some of it has been removed due to the threshold value of 0.18, which is on the high side. Therefore, the intensity pixel value of those important edges does not surpass the threshold value resulting in loss and un-linked edges which will give inaccurate readings on the feature points pixel coordinate. Table 4.6 shows the pixel coordinates and errors of each edge detection techniques with threshold value of 0.18.

Table 4.6 Edge detection with threshold value 0.18

Point	**Original Point (x, y pixel)**	**Identified Point (x, y pixel)**	**Error (Δx, Δy)**
Roberts edge detection with threshold value 0.18			
Start	789.0, 113.0	583.0, 286.5	205.0, 173.5
Supporting 1	574.0, 289.0	581.5, 291.0	-7.5, -2.0
Supporting 2	784.0, 459.0	583.0, 295.5	201, 163.5
End	576.0, 630.0	686.8, 381.6	-110.8, 248.4
Sobel edge detection with threshold value 0.18			
Start	789.0, 113.0	782.2, 125.3	6.8, 12.3
Supporting 1	574.0, 289.0	580.5, 290.4	-6.5, -1.4
Supporting 2	784.0, 459.0	734.9, 421.7	49.1, 32.3
End	576.0, 630.0	580.2, 622.6	-4.2, 7.4
Prewitt edge detection with threshold value 0.18			
Start	789.0, 113.0	783.2, 125.3	5.8, 12.3
Supporting 1	574.0, 289.0	580.5, 290.5	-6.5, -1.5
Supporting 2	784.0, 459.0	741.6, 423.6	42.4, 35.5
End	576.0, 630.0	780.6, 458.4	-204.6.171.6

4.3.2.2 Canny Edge Detection

Figure 4.7 shows the effect of low threshold value 0.2, 0.4, 0.6 and 0.8 towards Canny edge detection technique.

UNIVERSITI TEKNIKAL MALAYSIA MELAKA

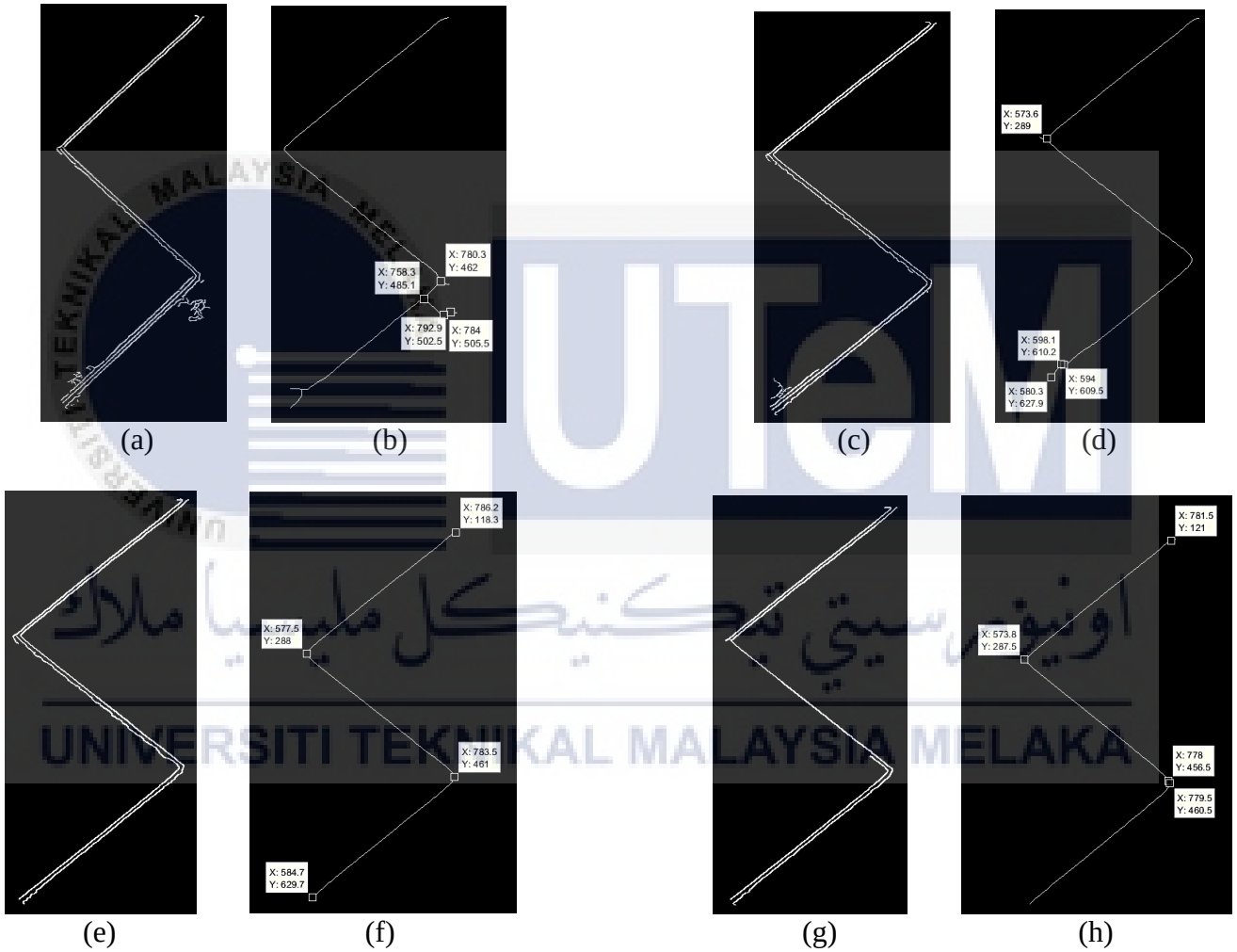

Figure 4.7 Low threshold value (a-b) 0.2 (c-d) 0.4 (e-f) 0.6 and (g-h) 0.8 on Canny edge detector

UNIVERSITI TEKNIKAL MALAYSIA MELAKA

From Figure 4.7, it can be observed that there is enough amount of information of the edge of tooth saw butt joint shape detected using threshold value (a-b) 0.2 and (c-d) 0.4 but, there is a small amount of unwanted edges that were taken into account as well. This is because the threshold values is too low causing some of the unwanted edges pixel intensity values are in between the range of the high and low threshold value, thus it is accepted as an important edges. Therefore, after image processing process, there are too many corners detected which causes errors in the feature points pixel coordinate readings. For threshold value (e-f) 0.6, there is a perfect amount of information of the edge of tooth saw butt joint shape detected and all the unwanted small edges has been successfully thresholded. This shows that the low threshold value of 0.6 is an optimal value of threshold because the intensity values of the unwanted edges are not able to surpass the low threshold value and being in the range of the high and low threshold value. Therefore, after image processing process, there is an optimum single straigth line and the corner detector able to detect the strongest and distinct points of the corners which is the feature points of the edge of the tooth saw butt joint shape. Threshold value (g-h) 0.8 removes some of the important edges from the edge of the tooth saw butt joint shape. This causes an error in image processing process in forming a single straight line using the morhpological dilation and skeletonization. The threshold value of 0.8 is too high causing it to also removes the important edges, where the intensity pixel values of those edges are unable to surpass the low threshold value resulting it to be defined as an un-important edges. Thus, the corner detector will have an error in detecting the strongest corners. Table 4.7 shows the coordinates of the feature points detected from using the low threshold value of 0.2, 0.4, 0.6, 0.8 and the error value towards the original points respectively.

Table 4.7 Canny edge detection with low threshold values 0.2, 0.4, 0.6 and 0.8

Point	Original Point (x, y pixel)	Identified Point (x, y pixel)	Error (Δx, Δy)
Canny edge detection with low threshold value 0.2			
Start	789.0, 113.0	780.3, 462.0	8.7, -349.0
Supporting 1	574.0, 289.0	758.3, 485.1	-184.3, 196.1
Supporting 2	784.0, 459.0	784.0, 505.5	0.0, 46.5
End	576.0, 630.0	792.9, 502.5	216.9, 127.5
Canny edge detection with low threshold value 0.4			
Start	789.0, 113.0	573.6, 289.0	215.0, -126.0
Supporting 1	574.0, 289.0	598.1, 610.2	-24.1, -321.2
Supporting 2	784.0, 459.0	594.0, 609.5	190.0. -150.5
End	576.0, 630.0	580.3 627.9	-4.3, 2.1
Canny edge detection with low threshold value 0.6			
Start	789.0, 113.0	786.2, 118.3	2.8, -5.3
Supporting 1	574.0, 289.0	577.5, 288.0	-3.5, 1.0
Supporting 2	784.0, 459.0	783.5, 461.0	-0.5, -2.0
End	576.0, 630.0	584.7, 629.7	-8.7, 0.3
Canny edge detection with low threshold value 0.8			
Start	789.0, 113.0	781.5, 121.0	7.5, -8.0
Supporting 1	574.0, 289.0	573.8, 287.5	0.2, 1.5
Supporting 2	784.0, 459.0	778.0, 456.5	6.0, 2.5
End	576.0, 630.0	779.5, 460.5	-203.5, 169.5

اونيۏرسيتي تيکنيکل مليسيا ملاک
UNIVERSITI TEKNIKAL MALAYSIA MELAKA

4.3.3 Validation of Structuring Element Size for Morphological Operation Dilation

Figure 4.8 and 4.9 shows the effects of the structuring element size for morphological operation dilation, which is the width of square of 40 and 30 pixels used for dilating the edges detected using Roberts, Sobel, Prewitt and Canny edge detector.

Figure 4.8 Dilation with square structuring element width of 40 pixels effects on (a-b) Roberts (c-d) Sobel (e-f) Prewitt and (g-h) Canny edge detector

UNIVERSITI TEKNIKAL MALAYSIA MELAKA

Figure 4.9 Dilation with square structuring element width of 30 pixels effects on (a-b) Roberts (c-d) Sobel (e-f) Prewitt and (g-h) Canny edge detector

UNIVERSITI TEKNIKAL MALAYSIA MELAKA

Based on Figure 4.8 and 4.9 it can be observed that the dilated image with structuring element size of 40 and 30 is too large for each edge detection techniques causing the final edges to lose its topological information on the original edges which means that it loses the sharp corner characteristic of supporting point 1 and 2 and becoming more curved-like, bending more inwards. Therefore, the corner detector, detects slightly different coordinates from the original edges. Table 4.8 shows the structuring element size of 40 and Table 4.9 shows the structuring element size of 30 which effects each of the edge detection techniques and the error value towards the original points respectively.

Table 4.8 Structuring element size of 40 pixel

Point	**Original Point (x, y pixel)**	**Identified Point (x, y pixel)**	**Error (Δx, Δy)**
Structuring element size of 40 pixel on Roberts edge detector			
Start	789.0, 113.0	588.0, 286.5	201.0, 174.5
Supporting 1	574.0, 289.0	586.5, 291.6	-12.5, -2.6
Supporting 2	784.0, 459.0	768.6, 462.5	-2.6, -3.5
End	576.0, 630.0	589.8, 818.7	-13.8, -188.7
Structuring element size of 40 pixel on Sobel edge detector			
Start	789.0, 113.0	764, 136.6	25.0, -23.6
Supporting 1	574.0, 289.0	587.1, 295.7	-13.1, -6.7
Supporting 2	784.0, 459.0	768.9, 468.7	15.1, -9.7
End	576.0, 630.0	590.7, 618.7	-14.7, 11.3
Structuring element size of 40 pixel on Prewitt edge detector			
Start	789.0, 113.0	764.5, 136.0	24.5, -23
Supporting 1	574.0, 289.0	586.6, 289.0	-12.6, 0.0
Supporting 2	784.0, 459.0	768.0, 470.5	16.0, -11.5
End	576.0, 630.0	591.2, 617.6	-15.2, 12.4
Structuring element size of 40 pixel on Canny edge detector			
Start	789.0, 113.0	584.5, 288.4	204.5, -175.4
Supporting 1	574.0, 289.0	585.1, 291.7	-11.1, -2.7
Supporting 2	784.0, 459.0	771.0, 451.5	13.0, 7.5
End	576.0, 630.0	770.0, 468.5	-194.0, 161.5

UNIVERSITI TEKNIKAL MALAYSIA MELAKA

Table 4.9 Structuring element size of 30 pixel

Point	Original Point (x, y pixel)	Identified Point (x, y pixel)	Error (Δx, Δy)
Structuring element size 30 on Roberts edge detector			
Start	789.0, 113.0	585.0, 287.5	204.0, -174.5
Supporting 1	574.0, 289.0	583.5, 291.5	-9.5, -2.5
Supporting 2	784.0, 459.0	770.5, 466.1	13.5, -7.1
End	576.0, 630.0	588.4, 620.6	-12.4, 9.4
Structuring element size 30 on Sobel edge detector			
Start	789.0, 113.0	581.0, 284.0	208.0, -171.0
Supporting 1	574.0, 289.0	584.1, 294.7	-10.1, -5.7
Supporting 2	784.0, 459.0	771.9, 458.3	12.1, 0.7
End	576.0, 630.0	771.0, 469.5	-195.0, 160.5
Structuring element size 30 on Prewitt edge detector			
Start	789.0, 113.0	769.5, 133.0	17.5, -20.0
Supporting 1	574.0, 289.0	585.9, 296.5	-11.9, -7.5
Supporting 2	784.0, 459.0	773.5, 463.0	10.5, -4.0
End	576.0, 630.0	585.2, 622.6	-9.2, 7.4
Structuring element size 30 on Canny edge detector			
Start	789.0, 113.0	781.7, 126.2	7.3, -13.2
Supporting 1	574.0, 289.0	768.5, 132.0	-194.5, 157.0
Supporting 2	784.0, 459.0	579.5, 291.4	204.5, 167.6
End	576.0, 630.0	771.5 464.4	-195.5, 165.6

Figure 4.10 and 4.11 shows the effects of the structuring element size for morphological operation dilation, which is the width of square of 20 and 10 pixels used for dilating the edges detected using Roberts, Sobel, Prewitt and Canny edge detector.

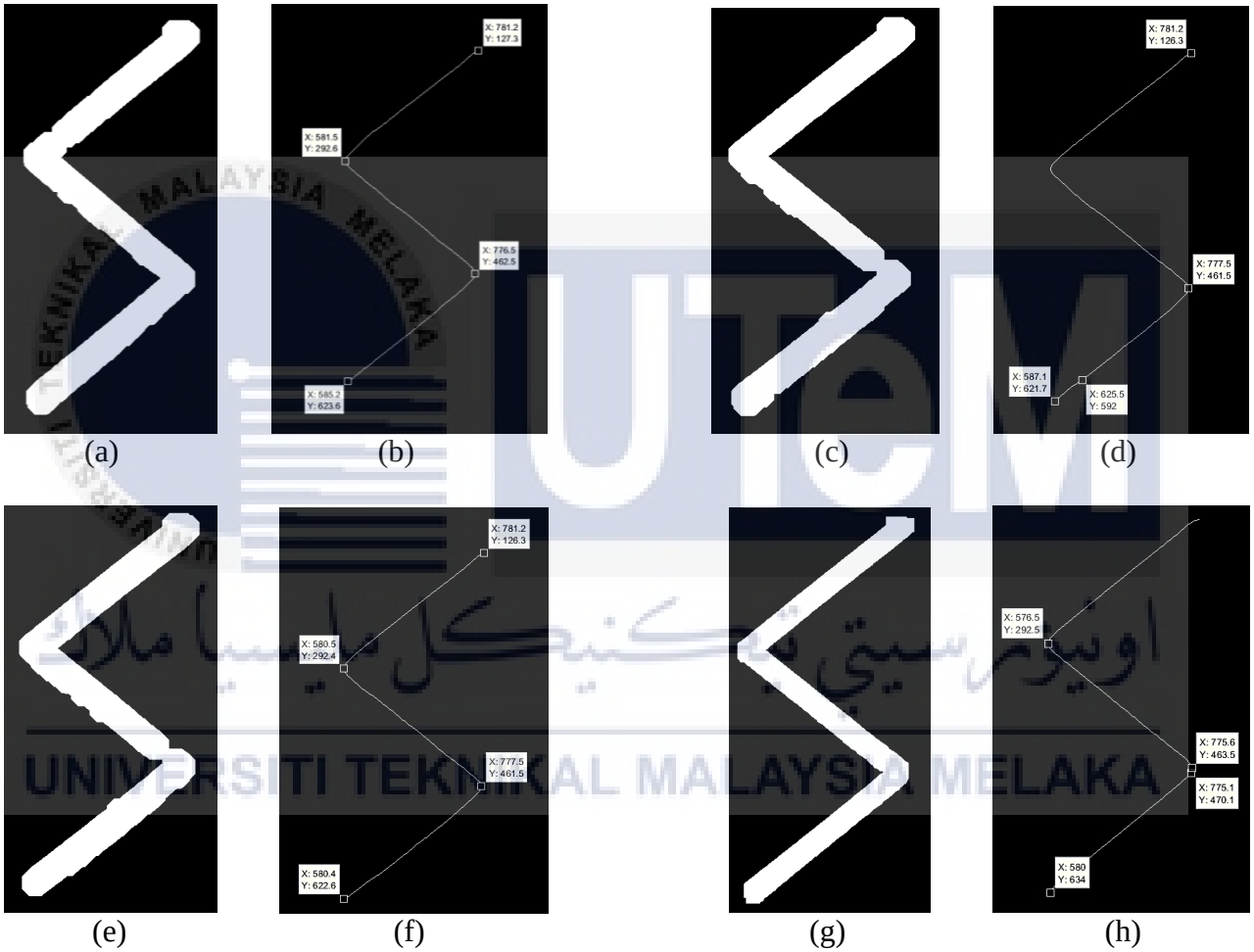

(a) (b) (c) (d)

(e) (f) (g) (h)

Figure 4.10 Dilation with square structuring element width of 20 pixels effects on (a-b) Roberts (c-d) Sobel (e-f) Prewitt and (g-h) Canny edge detector

UNIVERSITI TEKNIKAL MALAYSIA MELAKA

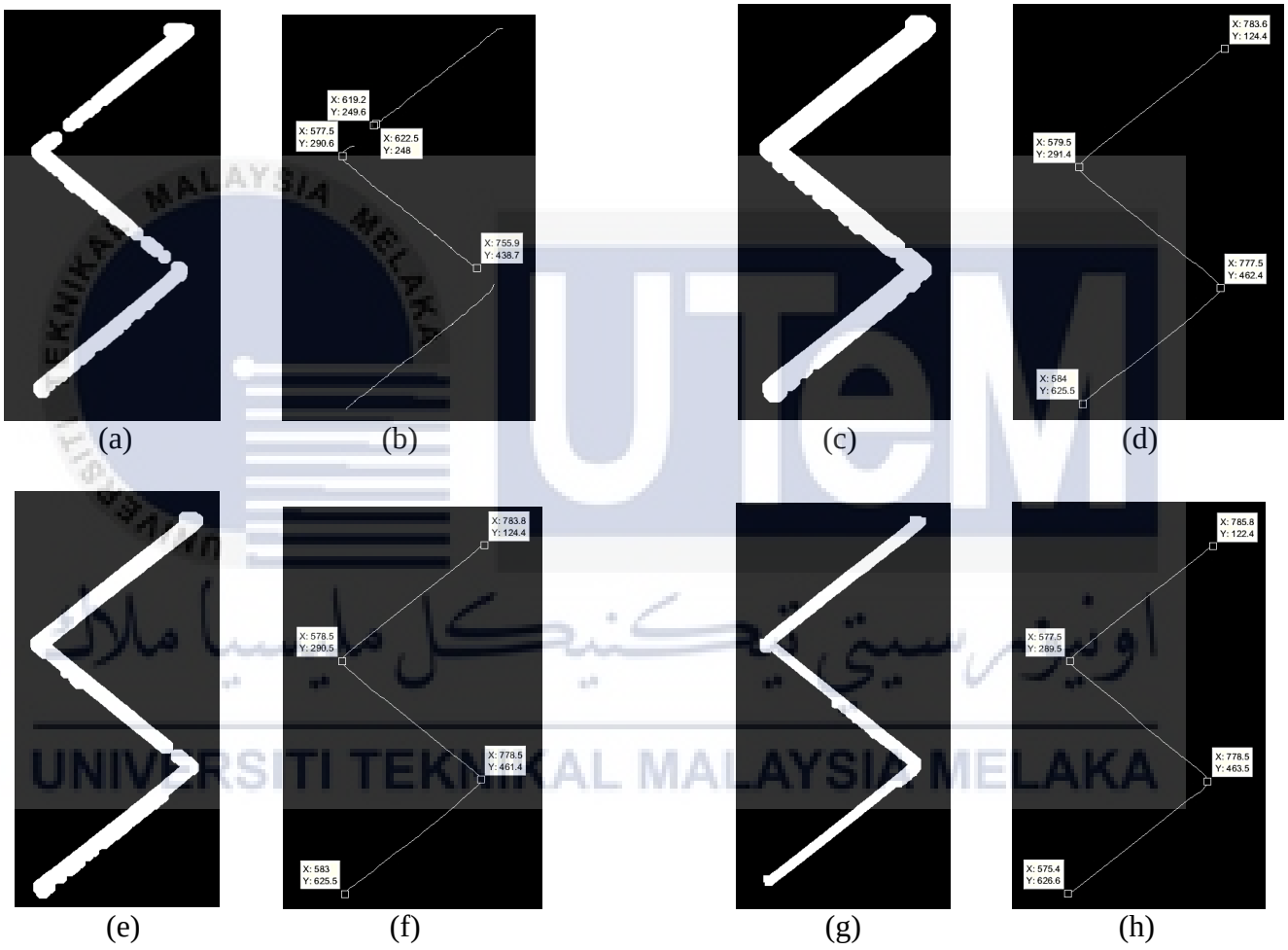

Figure 4.11 Dilation with square structuring element width of 10 pixels effects on (a-b) Roberts (c-d) Sobel (e-f) Prewitt and (g-h) Canny edge detector

UNIVERSITI TEKNIKAL MALAYSIA MELAKA

From Figure 4.10 and 4.11 it shows that, the most optimal value of dilation to combine the double edge line and the un-linked edges for (c-d) Sobel, (e-f) Prewitt and (g-h) Canny edge detector is by using a 10 pixel size structuring element. Although there are some edges that are nearly being un-linked for Sobel and Prewitt, but it does a good job in preserving the topological information of the original edge. For (a-b) Roberts edge detector, the size of 10 pixel is not suitable because there are some un-linked edges in the final image, thus high error in the coordinate pixel reading. The suitable size is 20 pixel eventhough the topological information of the original image has diminished, but it able to link all the un-linked edges forming an optimal single edge line. Table 4.10 shows the structuring element size of 20 and Table 4.11 shows the structuring element size of 10 which effects each of the edge detection techniques and the error value towards the original points.

Table 4.10 Structuring element size of 20 pixel

Point	**Original Point (x, y pixel)**	**Identified Point (x, y pixel)**	**Error (Δx, Δy)**
Structuring element size of 20 pixel on Roberts edge detector			
Start	789.0, 113.0	781.2, 127.3	7.8, -4.3
Supporting 1	574.0, 289.0	581.5, 292.6	-7.5, -3.6
Supporting 2	784.0, 459.0	776.5, 462.5	7.5, -3.5
End	576.0, 630.0	585.2, 623.6	-9.2, 6.4
Structuring element size of 20 pixel on Sobel edge detector			
Start	789.0, 113.0	781.2, 126.3	7.8, -13.3
Supporting 1	574.0, 289.0	777.5, 461.5	-203.5, -172.5
Supporting 2	784.0, 459.0	625.5, 592.0	158.5, 133.0
End	576.0, 630.0	587.1, 621.7	-11.1, 8.3
Structuring element size of 20 pixel on Prewitt edge detector			
Start	789.0, 113.0	781.2, 126.3	7.8, -13.3
Supporting 1	574.0, 289.0	580.5, 292.4	-6.5, -3.4
Supporting 2	784.0, 459.0	777.5, 461.5	6.5, -2.5
End	576.0, 630.0	580.4, 622.6	-4, 7.4
Structuring element size of 20 pixel on Canny edge detector			
Start	789.0, 113.0	576.5, 292.5	212.5, -179.5
Supporting 1	574.0, 289.0	775.6, 463.5	-201.6, -174.5
Supporting 2	784.0, 459.0	775.1, 470.1	8.9, -11.1
End	576.0, 630.0	580.0, 634.0	-4.0, -4.0

UNIVERSITI TEKNIKAL MALAYSIA MELAKA

Table 4.11 Structuring element size of 10 pixel

Point	Original Point (x, y pixel)	Identified Point (x, y pixel)	Error (Δx, Δy)
Structuring element size 10 on Roberts edge detector			
Start	789.0, 113.0	622.5, 248.0	166.5, -135
Supporting 1	574.0, 289.0	619.2, 249.6	-45.2, 39.4
Supporting 2	784.0, 459.0	577.5, 290.6	206.5, 168.4
End	576.0, 630.0	755.9, 438.7	-179.9, 191.3
Structuring element size 10 on Sobel edge detector			
Start	789.0, 113.0	783.6, 124.4	5.4, -11.4
Supporting 1	574.0, 289.0	579.5, 291.4	-5.5, -2.4
Supporting 2	784.0, 459.0	777.5, 462.4	6.4, -3.4
End	576.0, 630.0	584.0, 625.5	-8.0, 4.5
Structuring element size 10 on Prewitt edge detector			
Start	789.0, 113.0	783.8, 124.4	5.2, -11.4
Supporting 1	574.0, 289.0	578.5, 290.5	-4.5, -1.5
Supporting 2	784.0, 459.0	778.5, 461.4	5.5, -2.4
End	576.0, 630.0	583.0, 625.5	-7.0, 4.5
Structuring element size 10 on Canny edge detector			
Start	789.0, 113.0	785.8, 122.4	3.2, -9.4
Supporting 1	574.0, 289.0	577.5, 289.5	-4.5, -0.5
Supporting 2	784.0, 459.0	778.5, 463.5	5.5, -4.5
End	576.0, 630.0	575.4, 626.6	0.6, 3.4

UNIVERSITI TEKNIKAL MALAYSIA MELAKA

4.3.4 Validation of Corner Detection Minimum Quality

Figure 4.12, 4.13, 4.14 and 4.15 shows the various threshold for the minimum eigenvalues of the corner detection quality which are 0.1, 0.2, 0.3 and 0.4 used for the corners detection, Shi-Tomasi on the edge produced after image processing process and Table 4.12, 4.13, 4.14 and 4.15 shows the error values of the identified points on each of the edge detection techniques.

(a) (b) (c) (d)

(e) (f) (g) (h)

Figure 4.12 Minimum quality of corners with value 0.1 effects on (a-b) Roberts (c-d) Sobel (e-f) Prewitt and (g-h) Canny edge detector

UNIVERSITI TEKNIKAL MALAYSIA MELAKA

(a) (b) (c) (d)

(e) (f) (g) (h)

Figure 4.13 Minimum quality of corners with value 0.2 effects on (a-b) Roberts (c-d) Sobel (e-f) Prewitt and (g-h) Canny edge detector

UNIVERSITI TEKNIKAL MALAYSIA MELAKA

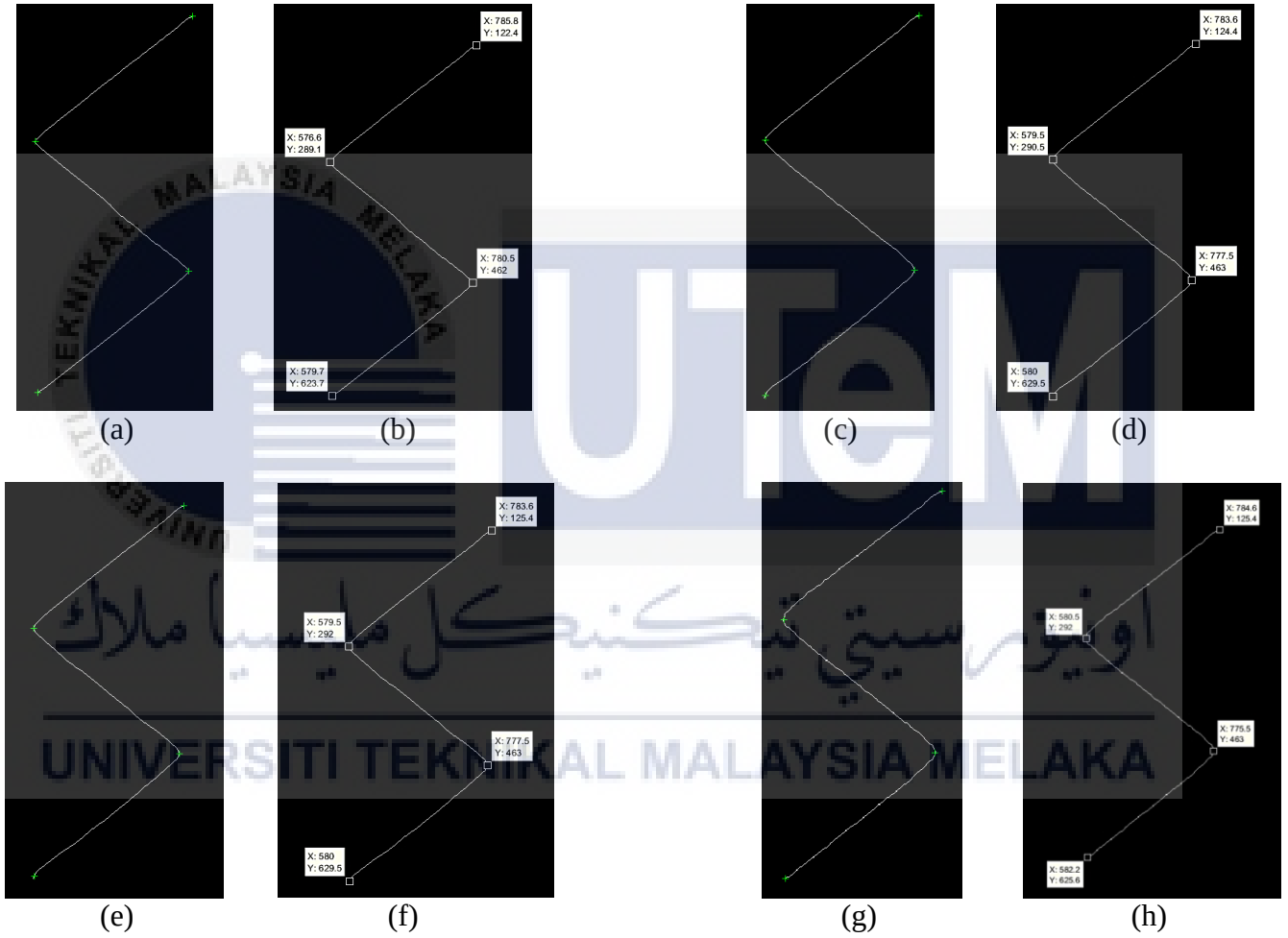

(a) (b) (c) (d)

(e) (f) (g) (h)

Figure 4.14 Minimum quality of corners with value 0.3 effects on (a-b) Roberts (c-d) Sobel (e-f) Prewitt and (g-h) Canny edge detector

UNIVERSITI TEKNIKAL MALAYSIA MELAKA

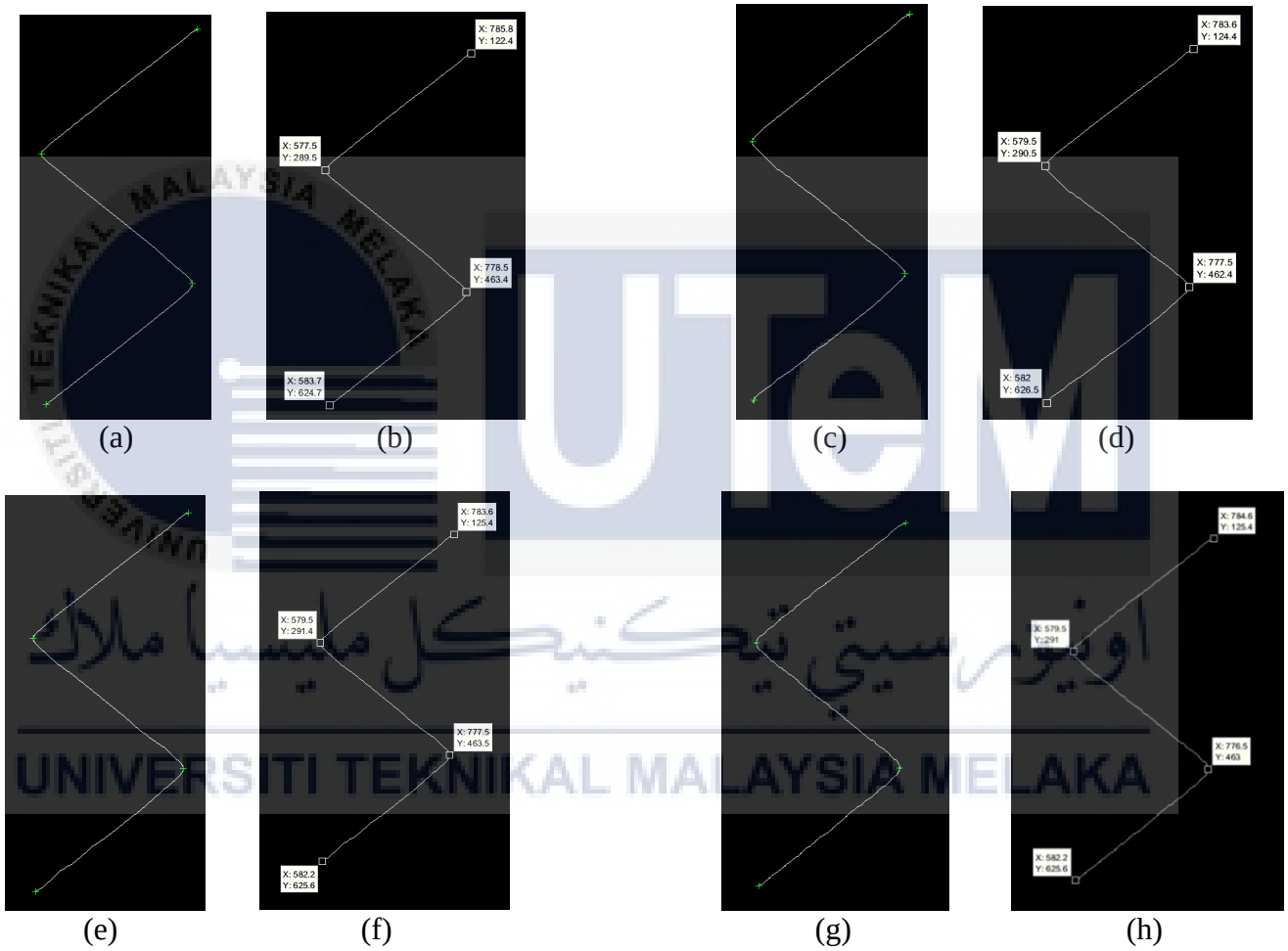

Figure 4.15 Minimum quality of corners with value 0.4 effects on (a-b) Roberts (c-d) Sobel (e-f) Prewitt and (g-h) Canny edge detector

UNIVERSITI TEKNIKAL MALAYSIA MELAKA

Table 4.12 Error values using minimum quality of 0.1

Point	Original Point (x, y pixel)	Identified Point (x, y pixel)	Error (Δx, Δy)
Minimum quality of corners value 0.1 on Roberts edge detector			
Start	789.0, 113.0	786.9, 124.3	2.1, -11.3
Supporting 1	574.0, 289.0	580.5, 293.5	-6.5, -4.5
Supporting 2	784.0, 459.0	777.5, 463.5	6.5, -4.5
End	576.0, 630.0	564.7, 624.7	11.4, 5.3
Minimum quality of corners value 0.1 on Sobel edge detector			
Start	789.0, 113.0	783.6, 125.4	5.5, 12.4
Supporting 1	574.0, 289.0	579.5, 292.6	-5.5, -3.6
Supporting 2	784.0, 459.0	775.5, 463.6	8.5, -4.6
End	576.0, 630.0	580.2, 623.6	-4.2, 6.4
Minimum quality of corners value 0.1 on Prewitt edge detector			
Start	789.0, 113.0	783.6, 124.4	5.4, -11.4
Supporting 1	574.0, 289.0	579.5, 291.4	-5.5, -2.4
Supporting 2	784.0, 459.0	777.5, 462.0	6.5, -3.0
End	576.0, 630.0	580.0, 629.5	-4.0, 0.5
Minimum quality of corners value 0.1 on Canny edge detector			
Start	789.0, 113.0	785.8, 122.4	3.2, -9.4
Supporting 1	574.0, 289.0	576.6, 289.1	-2.6, -0.1
Supporting 2	784.0, 459.0	777.5, 462.0	6.5, -3.0
End	576.0, 630.0	581.4, 625.6	-5.4, 4.4

Table 4.13 Error values using minimum quality of 0.2

Point	Original Point (x, y pixel)	Identified Point (x, y pixel)	Error (Δx, Δy)
Minimum quality of corners value 0.2 on Roberts edge detector			
Start	789.0, 113.0	786.9, 124.3	2.1, -11.3
Supporting 1	574.0, 289.0	580.5, 293.5	-6.5, -4.5
Supporting 2	784.0, 459.0	777.5, 463.5	6.5, -4.5
End	576.0, 630.0	564.7, 624.7	11.4, 5.3
Minimum quality of corners value 0.2 on Sobel edge detector			
Start	789.0, 113.0	783.6, 125.4	5.5, 12.4
Supporting 1	574.0, 289.0	579.5, 292.6	-5.5, -3.6
Supporting 2	784.0, 459.0	775.5, 463.6	8.5, -4.6
End	576.0, 630.0	580.2, 623.6	-4.2, 6.4
Minimum quality of corners value 0.2 on Prewitt edge detector			
Start	789.0, 113.0	783.6, 124.4	5.4, -11.4
Supporting 1	574.0, 289.0	579.5, 291.4	-5.5, -2.4
Supporting 2	784.0, 459.0	777.5, 462.0	6.5, -3.0
End	576.0, 630.0	580.0, 629.5	-4.0, 0.5

UNIVERSITI TEKNIKAL MALAYSIA MELAKA

Minimum quality of corners value 0.2 on Canny edge detector			
Start	789.0, 113.0	785.8, 122.4	3.2, -9.4
Supporting 1	574.0, 289.0	576.6, 289.1	-2.6, -0.1
Supporting 2	784.0, 459.0	777.5, 462.0	6.5, -3.0
End	576.0, 630.0	581.4, 625.6	-5.4, 4.4

Table 4.14 Error values using minimum quality of 0.3

Point	**Original Point (x, y pixel)**	**Identified Point (x, y pixel)**	**Error (Δx, Δy)**
Minimum quality of corners value 0.3 on Roberts edge detector			
Start	789.0, 113.0	786.9, 124.3	2.1, -11.3
Supporting 1	574.0, 289.0	580.5, 293.5	-6.5, -4.5
Supporting 2	784.0, 459.0	777.5, 463.5	6.5, -4.5
End	576.0, 630.0	564.7, 624.7	11.4, 5.3
Minimum quality of corners value 0.3 on Sobel edge detector			
Start	789.0, 113.0	783.6, 125.4	5.5, 12.4
Supporting 1	574.0, 289.0	579.5, 292.6	-5.5, -3.6
Supporting 2	784.0, 459.0	775.5, 463.6	8.5, -4.6
End	576.0, 630.0	580.2, 623.6	-4.2, 6.4
Minimum quality of corners value 0.3 on Prewitt edge detector			
Start	789.0, 113.0	783.6, 124.4	5.4, -11.4
Supporting 1	574.0, 289.0	579.5, 291.4	-5.5, -2.4
Supporting 2	784.0, 459.0	777.5, 462.0	6.5, -3.0
End	576.0, 630.0	580.0, 629.5	-4.0, 0.5
Minimum quality of corners value 0.3 on Canny edge detector			
Start	789.0, 113.0	785.8, 122.4	3.2, -9.4
Supporting 1	574.0, 289.0	576.6, 289.1	-2.6, -0.1
Supporting 2	784.0, 459.0	777.5, 462.0	6.5, -3.0
End	576.0, 630.0	581.4, 625.6	-5.4, 4.4

Table 4.15 Error values using minimum quality of 0.4

Point	**Original Point (x, y pixel)**	**Identified Point (x, y pixel)**	**Error (Δx, Δy)**
Minimum quality of corners value 0.4 on Roberts edge detector			
Start	789.0, 113.0	786.9, 124.3	2.1, -11.3
Supporting 1	574.0, 289.0	580.5, 293.5	-6.5, -4.5
Supporting 2	784.0, 459.0	777.5, 463.5	6.5, -4.5
End	576.0, 630.0	564.7, 624.7	11.4, 5.3
Minimum quality of corners value 0.4 on Sobel edge detector			
Start	789.0, 113.0	783.6, 125.4	5.5, 12.4
Supporting 1	574.0, 289.0	579.5, 292.6	-5.5, -3.6
Supporting 2	784.0, 459.0	775.5, 463.6	8.5, -4.6
End	576.0, 630.0	580.2, 623.6	-4.2, 6.4

UNIVERSITI TEKNIKAL MALAYSIA MELAKA

Minimum quality of corners value 0.4 on Prewitt edge detector			
Start	789.0, 113.0	783.6, 124.4	5.4, -11.4
Supporting 1	574.0, 289.0	579.5, 291.4	-5.5, -2.4
Supporting 2	784.0, 459.0	777.5, 462.0	6.5, -3.0
End	576.0, 630.0	580.0, 629.5	-4.0, 0.5
Minimum quality of corners value 0.4 on Canny edge detector			
Start	789.0, 113.0	785.8, 122.4	3.2, -9.4
Supporting 1	574.0, 289.0	576.6, 289.1	-2.6, -0.1
Supporting 2	784.0, 459.0	777.5, 462.0	6.5, -3.0
End	576.0, 630.0	581.4, 625.6	-5.4, 4.4

Overall, from the observation of figure 4.12, 4.13, 4.14, 4.15 and reading recorded on table 4.12, 4.13, 4.14 and 4.15, the optimal value of threshold for minimum pixel eigenvalues of the corner detection quality for all edge detection technique is 0.3. This is because it has a less error compared to the other values. This shows that the minimum pixel eigenvalues score of the pixel intensity value is greater than the threshold value of 0.3 to be depicted as a corner using the Shi-Tomasi corner detector on all of the edge detection techniques.

4.3.5 Identification of Feature Points

In this section, the original and final images containing the edge of the tooth saw butt joint shape that had underwent each of the digital image processing is shown, such as image before and after image pre-processing, image segmentation, morphological image processing and representation and description, using each of the edge detection techniques, Roberts, Sobel, Prewitt and Canny edge detector. This shows on how each of the digital image processing techniques effects the images and how it brings to the extraction of feature points of the edge of the tooth saw butt joint shape features. Lastly, the final identified feature points are presented in x and y coordinate pixel value. Figure 4.16, 4.17, 4.18 and 4.19 shows the process of digital image processing from the original image to the extraction of feature points of the edge of the tooth saw butt joint shape using each of the edge detection techniques.

UNIVERSITI TEKNIKAL MALAYSIA MELAKA

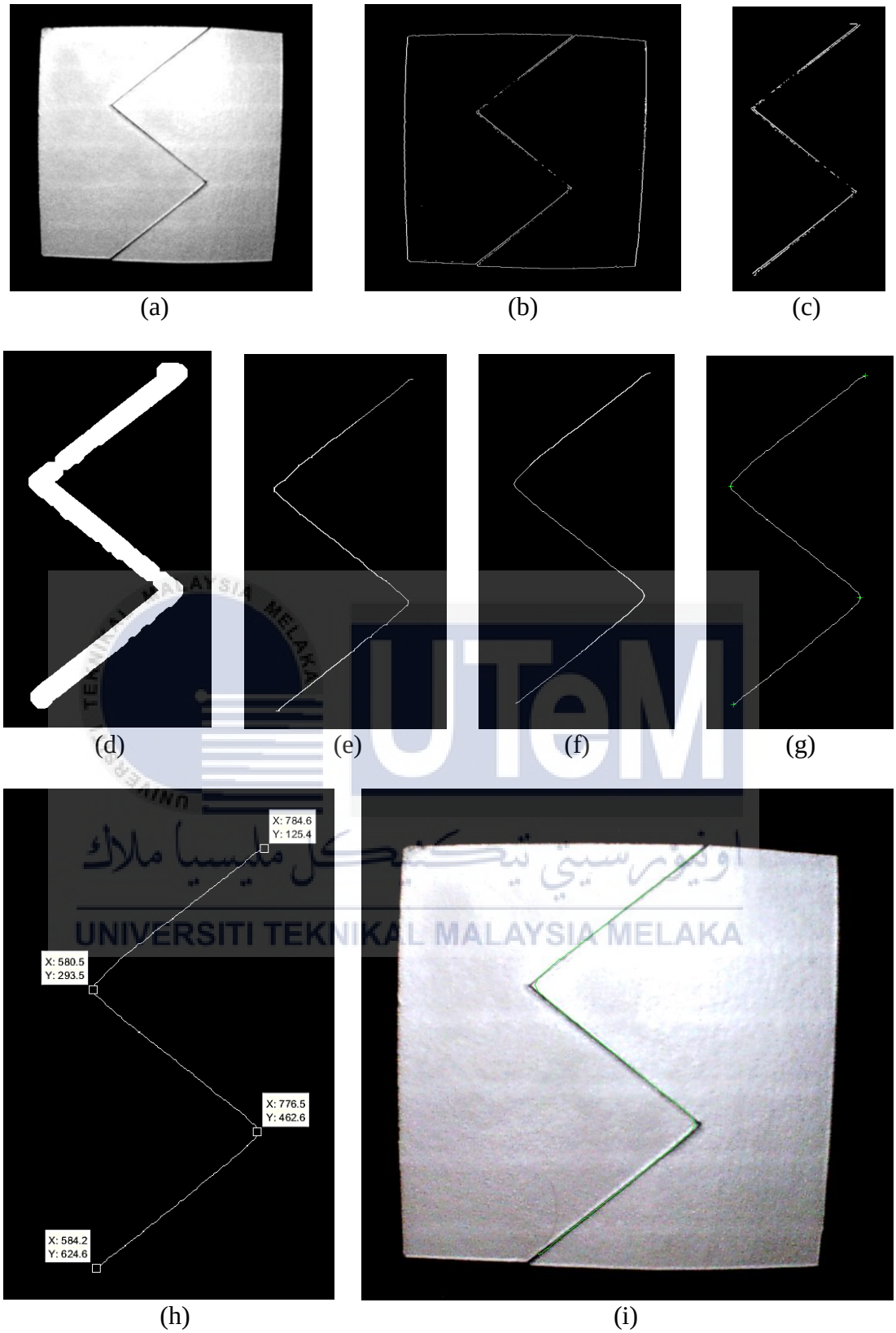

Figure 4.16 Image processing process (a) ROI image (b) Roberts Edge detection (c) Removal of unwanted edge (d) Dilated image (e) Skeletonized image (f) Smoothed image (g) Corner detected (h) Coordinates of corner detected (i) Detected edges traced on original Image

UNIVERSITI TEKNIKAL MALAYSIA MELAKA

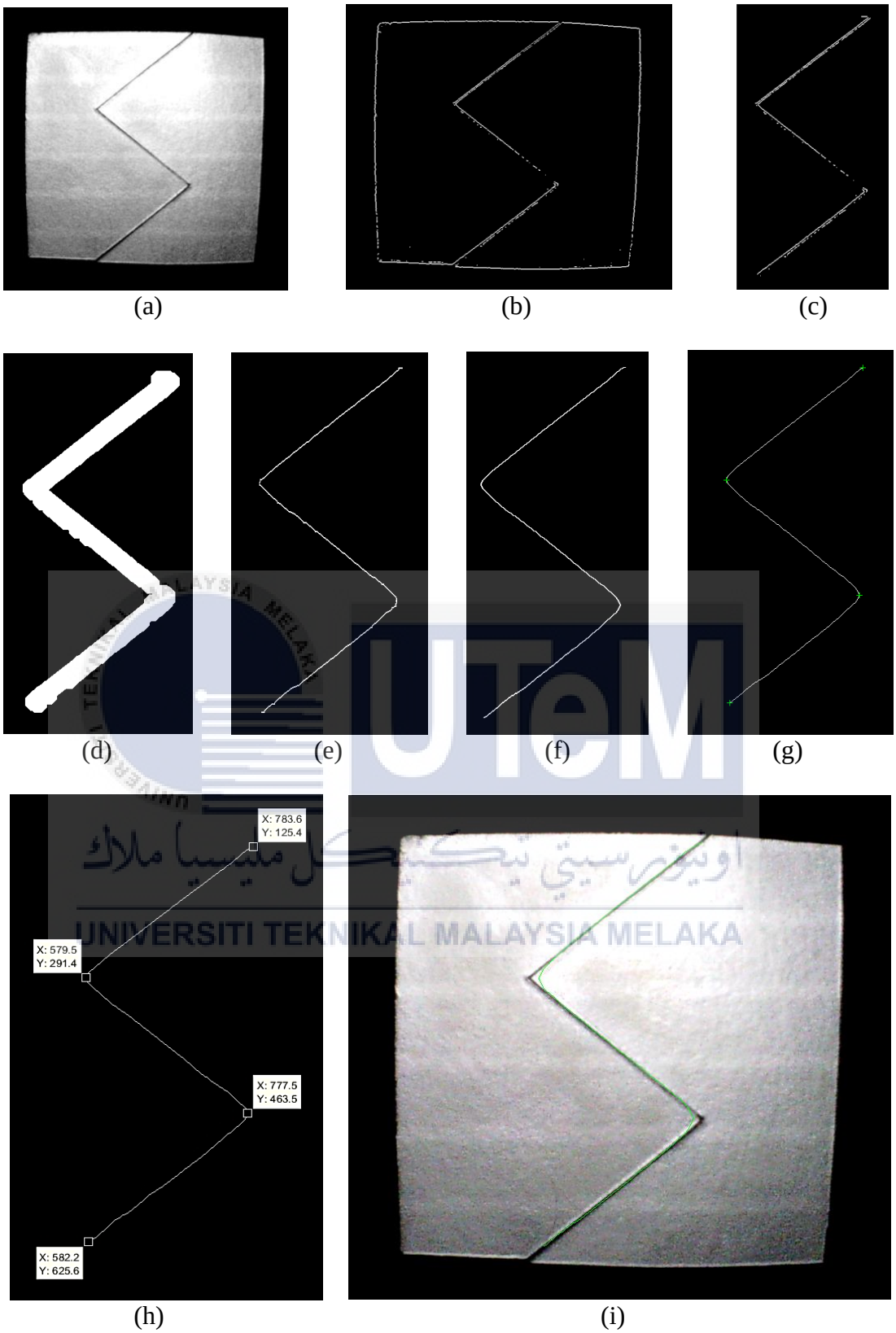

Figure 4.17 Image processing process (a) ROI image (b) Sobel Edge detection (c) Removal of unwanted edge (d) Dilated image (e) Skeletonized image (f) Smoothed image (g) Corner detected (h) Coordinates of corner detected (i) Detected edges traced on original Image

UNIVERSITI TEKNIKAL MALAYSIA MELAKA

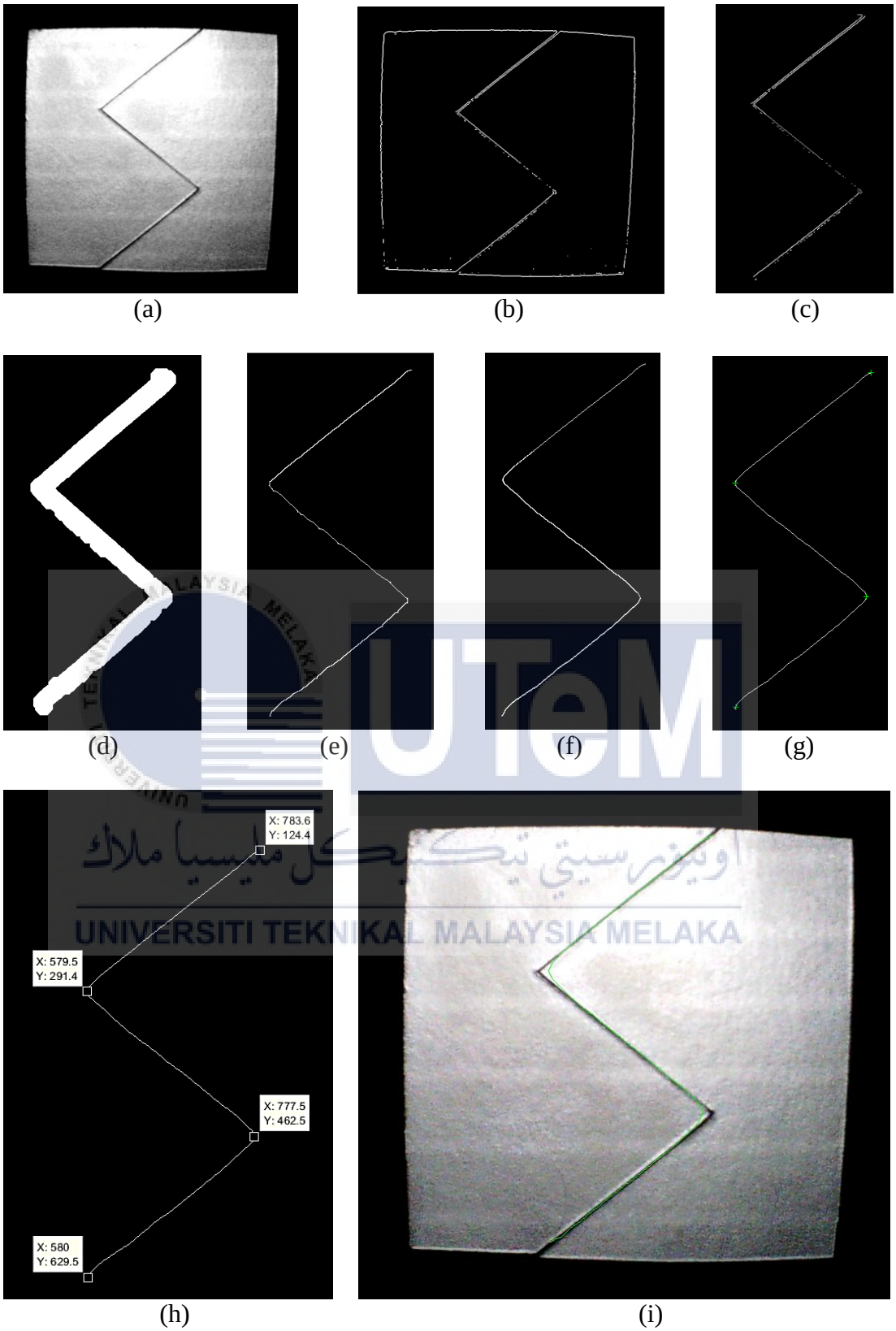

Figure 4.18 Image processing process (a) ROI image (b) Prewitt Edge detection (c) Removal of unwanted edge (d) Dilated image (e) Skeletonized image (f) Smoothed image (g) Corner detected (h) Coordinates of corner detected (i) Detected edges traced on original Image

UNIVERSITI TEKNIKAL MALAYSIA MELAKA

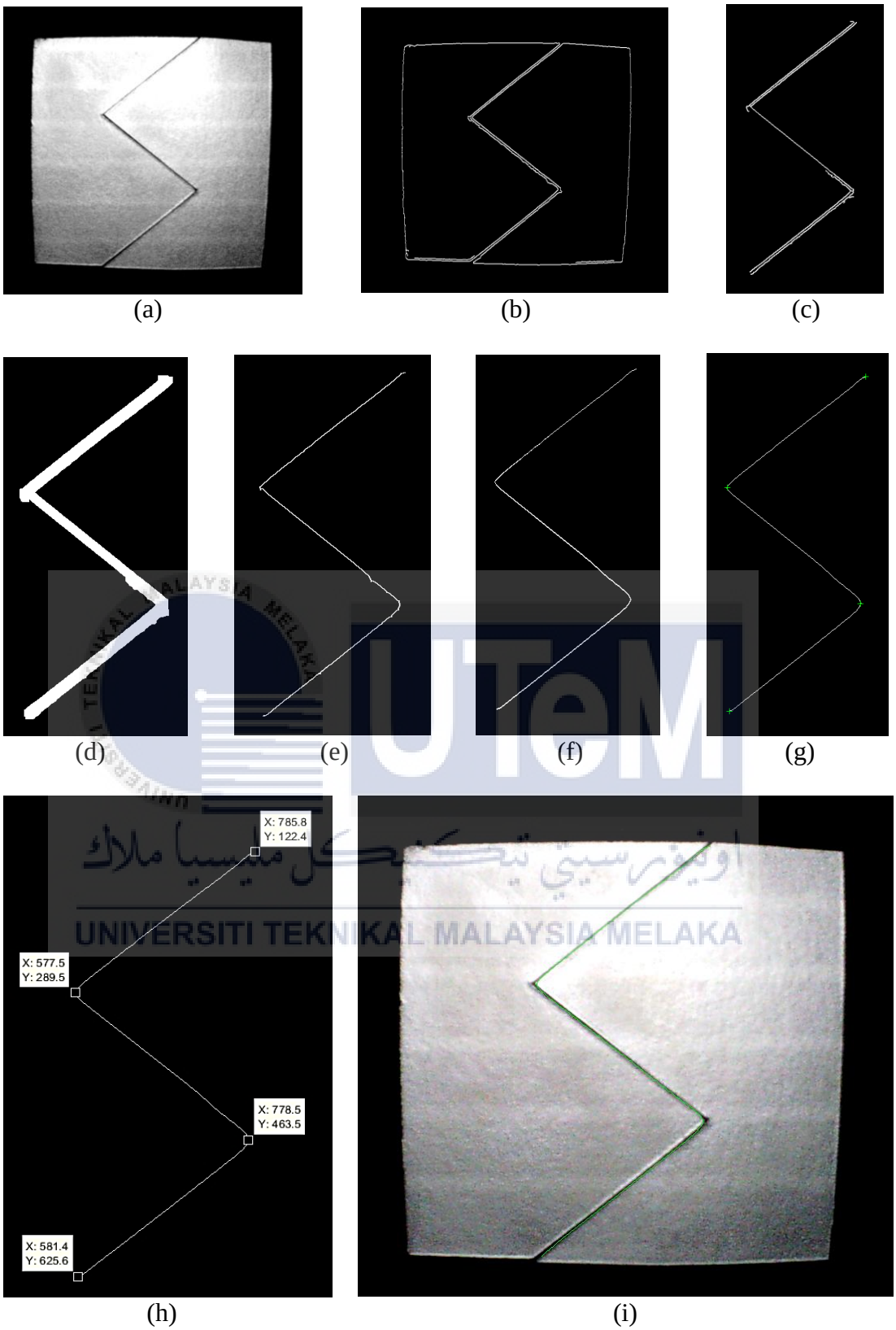

Figure 4.19 Image processing process (a) ROI image (b) Canny Edge detection (c) Removal of unwanted edge (d) Dilated image (e) Skeletonized image (f) Smoothed image (g) Corner detected (h) Coordinates of corner detected (i) Detected edges traced on original Image

UNIVERSITI TEKNIKAL MALAYSIA MELAKA

From Figure 4.16, 4.17, 4.18 and 4,19, image (a) in all of the figures shows the region of interest that had been applied to the original image to separate the work piece from the background to reduce the unwanted information inside the image. Image (b) in Figure 4.16 shows Roberts, Figure 4.17 shows Sobel, Figure 4.18 shows Prewitt and Figure 4.19 shows the Canny edge detection techniques that had been applied on image (a) using the selected pre-determined threshold value of 0.14 and 0.6 respectively. It shows that Canny edge detection technique has the highest sensitivity level in detecting the tooth saw edges. Then, image (c) in all of the figures shows the removal of the outer edge that is not needed using similar method as ROI isolation method. Image (d) in all figures shows the edge of the tooth saw butt joint shape being dilated to link all the un-linked edges and combine the double edges to form only a single line as shown in skeletonization and thinning process in image (e) and (f) in all figures using 20 pixels for Robert and 10 pixels for the rest of the edge detection techniques of width square structuring element size. The final edge formed is then used to detect the corners or the feature points of the tooth saw edge shape with a threshold of 0.3 for the minimum quality of eigenvalues of each pixel using every edge detection technique, shown in image (g) and (h) in all of the figures. Finally, image (i) shows the edge shape detected on top of the original image, where for Roberts has the most curved-like shape of the sharp corners due to the topological information loss during dilation process and Canny shows the sharpest corner in the edge detected. Table 4.16, 4.17, 4.18 and 4.19 shows the coordinates of the average identified points for ten readings in x and y pixel value using each of the edge detection techniques

UNIVERSITI TEKNIKAL MALAYSIA MELAKA

Table 4.16 Identified points using Roberts edge detection

Point	Identified Point (x, y pixel) Reading										Average reading (Mean, $\bar{x}$) (x, y pixel)
	1st	2nd	3rd	4th	5th	6th	7th	8th	9th	10th	
Start	784.6, 125.4	784.0, 125.4	784.4, 125.4	784.4, 125.4	784.6, 125.1	784.6, 125.1	784.6, 125.0	784.2, 125.4	784.3, 125.4	784.1, 125.4	784.4, 125.3
Supporting 1	580.5, 293.5	581.2, 292.1	581.1, 292.0	581.6, 292.9	580.9, 292.8	579.6, 293.6	579.58, 294.5	580.1, 294.7	580.1, 294.0	580.5, 294.0	580.5, 293.4
Supporting 2	776.5, 462.6	776.1, 463.1	776.1, 463.1	776.9, 464.6	775.5, 462.7	775.2, 461.8	775.1, 461.8	776.8, 462.0	774.9, 462.0	774.2, 462.3	775.7, 462.6
End	584.2, 624.6	584.5, 624.7	584.5, 624.6	584.6, 624.6	584.5, 624.6	584.3, 624.6	584.3, 624.2	584.3, 624.0	584.0, 624.0	584.1, 623.1	584.3, 624.3

Table 4.17 Identified points using Sobel edge detection

Point	Identified Point (x, y pixel) Reading										Average reading (Mean, $\bar{x}$) (x, y pixel)
	1st	2nd	3rd	4th	5th	6th	7th	8th	9th	10th	
Start	783.6, 125.4	783.6, 125.0	783.6, 125.0	783.1, 125.4	783.2, 125.5	783.2, 125.1	783.5, 125.3	783.5, 125.4	783.5, 125.4	783.4, 125.3	783.4, 125.3
Supporting 1	579.5, 291.4	579.0, 291.8	580.1, 292.0	577.5, 291.4	578.7, 291.4	579.1, 291.4	579.1, 290.9	578.9, 290.8	578.9, 289.9	579.0, 290.7	579.0, 291.2
Supporting 2	777.5, 463.5	776.7, 463.4	776.5, 463.5	777.9, 463.9	777.7, 464.2	778.0, 464.1	778.5, 464.0	776.9, 464.1	777.0, 463.5	777.0, 462.8	777.4, 464.0
End	582.2, 625.6	582.8, 625.7	581.6, 625.8	581.8, 625.1	582.4, 624.5	582.1, 624.7	582.2, 625.0	582.2, 625.0	582.4, 625.0	581.6, 625.1	582.1, 625.2

Table 4.18 Identified points using Prewitt edge detection

Point	Identified Point (x, y pixel) Reading										Average reading (Mean, $\bar{x}$) (x, y pixel)
	1st	2nd	3rd	4th	5th	6th	7th	8th	9th	10th	
Start	783.8, 124.4	783.8, 124.4	783.1, 124.4	783.8, 124.8	783.8, 122.1	784.0, 126.0	784.1, 124.4	783.2, 124.3	783.2, 124.8	783.9, 124.4	783.7, 124.4
Supporting 1	579.5, 291.4	580.2, 291.2	579.2, 289.0	576.9, 292.1	578.7, 291.6	579.3, 291.4	579.3, 291.4	579.5, 291.4	579.5, 291.8	578.9, 292.0	579.1, 291.4
Supporting 2	777.5, 462.5	778.1, 462.3	777.5, 462.5	777.5, 462.5	776.3, 462.5	776.9, 462.7	777.2, 463.1	778.2, 461.8	777.1, 461.5	777.6, 462.0	777.4, 463.1
End	580.0, 629.0	580.2, 629.5	580.2, 629.2	581.0, 628.9	580.0, 629.1	580.0, 629.1	580.5, 629.3	580.0, 629.5	580.3, 629.5	581.2, 629.1	580.3, 629.3

Table 4.19 Identified points using Canny edge detection

Point	Identified Point (x, y pixel) Reading										Average reading (Mean, $\bar{x}$) (x, y pixel)
	1st	2nd	3rd	4th	5th	6th	7th	8th	9th	10th	
Start	785.8, 122.4	785.8, 122.4	785.8, 122.4	785.8, 122.4	785.8, 122.4	785.8, 122.4	785.8, 122.4	785.8, 122.4	785.8, 122.4	785.8, 122.4	785.8, 122.4
Supporting 1	577.5, 289.5	577.0, 288.7	577.8, 288.5	576.5, 288.4	575.1, 289.1	579.2, 289.1	574.5, 289.2	575.9, 289.9	577.3, 290.2	577.1, 289.7	576.8, 289.2
Supporting 2	778.5, 463.5	777.5, 460.1	778.3, 463.2	777.2, 464.2	779.1, 463.8	778.2, 463.8	778.7, 461.7	779.2, 463.7	779.1, 465.1	778.1, 463.2	778.4, 463.2
End	581.4, 625.6	581.4, 625.6	581.4, 625.6	581.4, 625.6	581.5, 625.6	581.4, 625.6	581.5, 625.6	581.4, 625.6	582.4, 625.6	581.4, 625.6	581.5, 625.6

4.4 Experiment 2: Accuracy Test

In this accuracy test, the difference between the mean value for each identified start point, supporting point 1 & 2 and end point and the original point for each edge detection techniques used is compared with the original feature points of the edge of the tooth saw butt joint shape. The value is in x and y coordinate pixel value. If the difference or the error value is nearing to zero, thus the proposed method has a high accuracy. If the difference or the error value is furthering from zero, thus the proposed method has a low accuracy. Table 4.20 shows the accuracy test for Canny, Prewitt, Sobel and Roberts edge detection technique.

Table 4.20 Accuracy Test

Point	**Original Point (x, y pixel)**	**Identified Point (Mean, $\bar{x}$) (x, y pixel)**	**Error (Δx, Δy)**
Roberts edge detection accuracy test			
Start	789.0, 113.0	784.4, 125.3	4.6, -12.3
Supporting 1	574.0, 289.0	580.5, 293.4	-6.5, -4.4
Supporting 2	784.0, 459.0	775.7, 462.6	8.3, 3.6
End	576.0, 630.0	584.3, 624.3	-8.3, 5.7
Sobel edge detection accuracy test			
Start	789.0, 113.0	783.4, 125.3	5.6, -12.3
Supporting 1	574.0, 289.0	579.0, 291.2	-5.0, -2.2
Supporting 2	784.0, 459.0	777.4, 464.0	6.6, -5.0
End	576.0, 630.0	582.1, 625.2	-6.1, 4.8
Prewitt edge detection accuracy test			
Start	789.0, 113.0	783.7, 124.4	5.3, -11.4
Supporting 1	574.0, 289.0	579.1, 291.4	-5.1, -2.4
Supporting 2	784.0, 459.0	777.4, 463.1	6.6, -4.1
End	576.0, 630.0	580.3, 629.3	-4.3, 0.7
Canny edge detection accuracy test			
Start	789.0, 113.0	785.8, 122.4	3.2, -9.4
Supporting 1	574.0, 289.0	576.8, 289.2	-2.8, -0.2
Supporting 2	784.0, 459.0	778.4, 463.2	5.6, -4.2
End	576.0, 630.0	581.5, 625.6	-5.5, 4.4

Based on Table 4.20, it shows that the overall error value for Canny edge detector in the identification of the start point, supporting point 1 & 2 and the end point pixel coordinates is the least compared to the other three edge detection techniques. This shows that the Canny edge detector has a high accuracy in detecting edges. This

is due to the hysteresis threshold where two thresholds that is pre-determined, which add more definition to the edge detection. Next, Prewitt edge detector shows a low value of error compared to Sobel and Roberts edge detection techniques eventhough three of those techniques use similar method where one threshold is predetermined in order to detect the edges. This is because the kernel used in Prewitt has better performance in determining the magnitude of the gradient in the image that contains the edges, compared to Sobel and Roberts edge detectors. Therefore, among the three edge detection techniques, Canny edge detector has a highest accuracy in finding important edges.

4.5 Experiment 3: Repeatability Test

In this repeatability test, the average reading of the identified start point, supporting point 1 & 2 and end point for the image containing the edge of the tooth saw butt joint shape is used to calculate the standard deviation of each edge detection method. The value of standard deviation is used to determine the repeatability of each method, where low value of standard deviation shows that each ten reading taken to find the average reading has low variations between them. Therefore, the method and variables used to obtain the reading has a high repeatability and reliability to obtain a reading near the average reading. Table 4.21 shows the standard deviation of each edge detection technique, Canny, Prewitt, Sobel and Roberts Edge detector.

UNIVERSITI TEKNIKAL MALAYSIA MELAKA

Table 4.21 Repeatability test

Point	**Average reading, (Mean, $\bar{x}$), (x, y pixel)**	**Standard Deviation, s**
Roberts edge detector standard deviation		
Start	784.4, 125.3	0.4, 0.0
Supporting 1	580.5, 293.4	0.0, 0.4
Supporting 2	775.7, 462.6	1.6, 0.2
End	584.3, 624.3	0.1, 1.1
Sobel edge detector standard deviation		
Start	783.4, 125.3	0.1, 0.1
Supporting 1	579.0, 291.2	0.4, 0.5
Supporting 2	777.4, 464.0	0.4, 0.5
End	582.1, 625.2	0.4, 0.4

Prewitt edge detector standard deviation		
Start	783.7, 124.4	0.1, 0.0
Supporting 1	579.1, 291.4	0.4, 0.4
Supporting 2	777.4, 463.1	0.1, 0.4
End	580.3, 629.3	0.8, 0.1
Canny edge detector standard deviation		
Start	785.8, 122.4	0.0, 0.0
Supporting 1	576.8, 289.2	0.3, 0.1
Supporting 2	778.4, 463.2	0.3, 0.2
End	581.5, 625.6	0.0, 0.0

Based on Table 4.21, it shows that all the edge detection techniques have a low value of standard deviation nearing 0. Each reading of the coordinates of the feature points is near to its average reading, thus, low in variations. This proves that the procedure used and the determined variables for each edge detection techniques shows a high repeatability and reliability, meaning that the repeated reading on the coordinates of the features points using the same equipment, procedures, methods and variables has less spread from the average reading.

4.6 Chapter Summary

For the preliminary task, the reference point has been marked using human observation from the original image captured without any image processing applied to it. The pixel coordinates of the marked points are determined based on the starting point, the corners of the edge of the tooth saw butt joint shape and the ending point. Other points are also marked, such as ROI 1 and ROI 2 to filter unwanted information and to remove unwanted edges respectively. In between the process of experiment 1, which is to identify the feature points of the edge, validation on the variables are analyzed. Overall, for the illumination brightness, 10 lumen shows the most optimal image quality without any over-exposure and each of the edge detector, Canny, Prewitt, Sobel and Roberts are able to detect enough information of the edge of the tooth saw butt joint shape. For the threshold value of the edge detectors, the most optimal value of threshold for Prewitt, Sobel and Roberts edge detector are 0.14 and value of threshold for Canny edge detector is 0.6. From those threshold values, the edge detectors able to convert the orginal image to binary image, and detect the discontinuity boundaries of the edges well. After the edge detection, morphological operation dilation is applied to link un-linked edges and combine double edges with

UNIVERSITI TEKNIKAL MALAYSIA MELAKA

the optimal width for the square structuring element, which is 10 pixels for Canny, Prewitt and Sobel, and 20 pixels for Roberts edge detection technique. From the final edges produced, the optimal value of threshold for minimum pixel eigenvalues of the corner detection quality is analyzed with a value 0.3 for all edge detection techniques. This is because the strength of corners detected shows a nearly accurate reading towards the original points. The edge recognized are compared to the original edge of the tooth saw butt joint shape. It shows that Roberts has a more curved-like shape on the sharp corners due to the large structuring element size for dilation operation and Canny has the most similar shape to the original tooh saw edge shape. Finally, for experiment 2 and 3, the evaluation shows that Canny edge detection technique has the lowest error in identifying the feature points of the edges which proves that it is the most optimal solution in finding discontinuities boundary of an edge and every edge detection techniques exhibit a low value of standard deviation showing that the methods, variables determined and procedure done has high realibility in producing results near the average reading.

UTeM
اونيۏرسيتي تيکنيکل مليسيا ملاک
UNIVERSITI TEKNIKAL MALAYSIA MELAKA

CHAPTER 5

CONCLUSION AND RECOMMENDATION

5.1 Conclusion

Based on the results and evaluations obtained in Chapter 4 of this thesis project, the first objective, which is to develop a vision-based method in recognizing the edge of a tooth saw butt joint shape has been achieved by using digital image processing and different edge detection techniques, which are Canny, Prewitt, Sobel and Roberts edge detectors. After the first objective is achieved, further digital image processing, such as morphological operation and feature points extraction, Shi-Tomasi corner detector are applied to achieve the second objective which is to identify the feature points of the recognized edges. The process in identifying the feature points of the recognized edges is repeated ten times to obtain an average reading, which helps in reducing errors, using all the edge detection techniques. For the third objective, which is to evaluate the accuracy of the identified feature points compared to its actual feature points, the average reading of each edge detection techniques are compared with the actual feature points. Canny edge detector shows the highest accuracy in detecting the feature points of the edge of a tooth saw butt joint shape due to the hysteresis threshold of the edge detector which is a two pre-determined threshold value that gives more definition to the edge detected, followed by Prewitt, Sobel and Roberts edge detector. Before all of the edge detection techniques can be applied, the analysis had been successfully made on the validation of illumination brightness, threshold value, width of the square structuring element for morphological operation dilation and the threshold for the minimum quality of pixel in the image to give the methods the accuracy to detect the edges. Thus, the third objective had been successfully achieved. Finally, for the last objective, which is to evaluate the repeatability of the developed methods in identifying the feature points of the edge of a tooth saw butt joint shape, it shows that with all the pre-determined variable used and the procedure done in order to obtain the feature points of the edge of the tooth saw butt joint shape, each of the edge detection techniques has a low value of standard deviation. It shows that, the repeated reading obtain for each of the edge detection techniques has a low variation in its readings,

UNIVERSITI TEKNIKAL MALAYSIA MELAKA

meaning that the methods have a high repeatability and reliability on the procedures and variables used. Thus, the repeatability of each edge detection techniques has been successfully evaluated.

5.2 Recommendation

The work piece in this project is made from a hard cardboard material and spray painted with silver colour to imitate the reflective behaviour of an aluminium sheet. That work piece is used because of its availability and easy to handle, meaning that it is easily obtained and the work piece can be easily cut to obtained the shape of a tooth saw butt joint. It is recommended for future work to use a real aluminium sheet or any mild steel to perform this project to exhibit the real characteristic behaviour of those materials because the application of this project is used in industrial robotic welding. In terms of industrial robotic welding, this project can also be further integrated with a robot arm by calibrating the vision system to convert the coordinates of the identified feature points of the work piece to coordinates of the robot path using inverse kinematics. Next, for future studies, comparison can be made more by using different shape of butt joint edges, such as straight line, curved and even a higher number of sharp edges of a tooth saw shape. This is to test out the effectiveness of the edge and corner detection techniques proposed in this project. In terms of method used, further comparison can also be made using different edge and corner detection techniques, such as adaptive thresholding and Harris corner detector method respectively to overcome the limitation of doing this project in a controlled environment.

UNIVERSITI TEKNIKAL MALAYSIA MELAKA

REFERENCES

[1] J. D. L. E.N. Malamas, E.G.M. Petrakis, M. Zervakis, L. Petit, "A survey on industrial vision systems,applications and tools, Image and Vision Computing," *Image Vis. Comput.*, vol. 21, no. 2, pp. 171–188, 2003.

[2] H. Golnabi and A. Asadpour, "Design and application of industrial machine vision systems," *Robot. Comput. Integr. Manuf.*, vol. 23, no. 6, pp. 630–637, 2007.

[3] A. Rout, B. B. V. L. Deepak, and B. B. Biswal, "Advances in weld seam tracking techniques for robotic welding: A review," *Robot. Comput. Integr. Manuf.*, vol. 56, no. August 2018, pp. 12–37, 2019.

[4] H. N. M. Shah, M. Sulaiman, A. Z. Shukor, Z. Kamis, and A. A. Rahman, "Butt welding joints recognition and location identification by using local thresholding," *Robot. Comput. Integr. Manuf.*, vol. 51, no. December 2017, pp. 181–188, 2018.

[5] M. Dinham and G. Fang, "Autonomous weld seam identification and localisation using eye-in-hand stereo vision for robotic arc welding," *Robot. Comput. Integr. Manuf.*, vol. 29, no. 5, pp. 288–301, 2013.

UNIVERSITI TEKNIKAL MALAYSIA MELAKA

[6] Y. He, Y. Xu, Y. Chen, H. Chen, and S. Chen, "Weld seam profile detection and feature point extraction for multi-pass route planning based on visual attention model," *Robot. Comput. Integr. Manuf.*, vol. 37, pp. 251–261, 2016.

[7] J. Carroll. (2015, August 25). Machine vision industry in Germany reached record numbers in 2015 [Online]. Available: https://www.vision-systems.com/articles/2016/08/machine-vision-industry-in-germany-reached-record-numbers-in-2015.html

[8] A. Martin and S. Tosunoglu, "Image Processing Techniques For Machine Vision," *Miami, Florida*, pp. 1–9, 2000.

[9] N. Alfaraj, “A review of charge-coupled device image sensors A Review of Charge-Coupled Device Image Sensors,” no. February, 2017.

[10] M. Bigas, E. Cabruja, J. Forest, and J. Salvi, “Review of CMOS image sensors,” *Microelectronics J.*, vol. 37, no. 5, pp. 433–451, 2006.

[11] Stemmer Imaging L.t.d. (2018). Illumination techniques for industrial image processing [Online]. Available: https://www.stemmer-imaging.com/en-gb/technical-tips/illumination-techniques/

[12] R. C. Gonzalez and R. E. Woods, “Introduction to Digital Image Processing” in *Digital Image Processing, 2nd* ed. Upper Saddle River, New Jersey 07458, 202, ch. *1*, sec. *1*, pp 1-2

[13] B. G. Batchelor and F. M. Waltz, “Morphological image processing,” *Mach. Vis. Handb.*, vol. 8491, pp. 802–870, 2012.

[14] D. Kaur and Y. Kaur, “Various Image Segmentation Techniques: A Review,” *Int. J. Comput. Sci. Mob. Comput.*, vol. 3, no. 5, p. 809–814, date accessed: 18/05/2016, 2014.

UNIVERSITI TEKNIKAL MALAYSIA MELAKA

[15] K. Bala Krishnan, S. Prakash Ranga, and N. Guptha, “A Survey on Different Edge Detection Techniques for Image Segmentation,” *Indian J. Sci. Technol.*, vol. 10, no. 4, 2017.

[16] Y. Zou, Y. Wang, W. Zhou, and X. Chen, “Real-time seam tracking control system based on line laser visions,” *Opt. Laser Technol.*, vol. 103, pp. 182–192, 2018.

[17] Y. Xu *et al.*, “Welding seam tracking in robotic gas metal arc welding,” *J. Mater. Process. Technol.*, vol. 248, no. May, pp. 18–30, 2017.

[18] W. J. Shao, Y. Huang, and Y. Zhang, “A novel weld seam detection method for space weld seam of narrow butt joint in laser welding,” *Opt. Laser Technol.*, vol. 99, pp. 39–51, 2018.

[19] Y. Zou, X. Chen, G. Gong, and J. Li, “A seam tracking system based on a laser vision sensor,” *Meas. J. Int. Meas. Confed.*, vol. 127, no. February, pp. 489–500, 2018.

[20] J. Fan, F. Jing, L. Yang, T. Long, and M. Tan, “A precise seam tracking method for narrow butt seams based on structured light vision sensor,” *Opt. Laser Technol.*, vol. 109, no. 95, pp. 616–626, 2019.

[21] J. Zeng, B. Chang, D. Du, Y. Hong, Y. Zou, and S. Chang, “A visual weld edge recognition method based on light and shadow feature construction using directional lighting,” *J. Manuf. Process.*, vol. 24, pp. 19–30, 2016.

[22] H. N. M. Shah, M. Sulaiman, A. Z. Shukor, and M. Z. A. Rashid, “Vision Based Identification and Detection of Initial , Mid and End Points of Weld Seams Path in Butt- Welding Joint using Point Detector Methods,” vol. 8, no. 7, pp. 57–61, 1843.

[23] S. Javier and N. Monz, “An Analysis and Implementation of the Harris Corner Detector The Harris Corner Detector,” vol. 8, pp. 305–328, 2018.

[24] Ghandi, N. (2018, July 24). Harris Corner Detection and Shi-Tomasi Corner Detection [Online]. Available: https://medium.com/pixel-wise/detect-those-corners-aba0f034078b

UNIVERSITI TEKNIKAL MALAYSIA MELAKA

[25] W. Abu-ain, S. Norul, H. Sheikh, B. Bataineh, T. Abu-ain, and K. Omar, “Skeletonization Algorithm for Binary Images,” *Procedia Technol.*, vol. 11, no. Iceei, pp. 704–709, 2013.

[26] P. Xu, X. Tang, and S. Yao, “Application of circular laser vision sensor (CLVS) on welded seam tracking,” *J. Mater. Process. Technol.*, vol. 205, no. 1–3, pp. 404–410, 2008.

[27] H. N. M. Shah, M. Sulaiman, A. Z. Shukor, and Z. Kamis, “Recognition and identification the position and location of tooth saw butt joint shape,” *Int. J. Adv. Manuf. Technol.*, vol. 98, no. 9–12, pp. 2497–2504, 2018.

[28] E. Tournas and M. Tsakiri, “Distance Error Estimation for Range Imaging Sensors,” *Archives*, vol. XXXVIII, 2010.

[29] M. Nilsen, F. Sikström, A. K. Christiansson, and A. Ancona, “Monitoring of Varying Joint Gap Width during Laser Beam Welding by a Dual Vision and Spectroscopic Sensing System,” *Phys. Procedia*, vol. 89, pp. 100–107, 2017.

[30] M. Nilsen, F. Sikström, A. K. Christiansson, and A. Ancona, “Vision and spectroscopic sensing for joint tracing in narrow gap laser butt welding,” *Opt. Laser Technol.*, vol. 96, pp. 107–116, 2017.

[31] Y. Xu, G. Fang, N. Lv, S. Chen, and J. Jia Zou, “Computer vision technology for seam tracking in robotic GTAW and GMAW,” *Robot. Comput. Integr. Manuf.*, vol. 32, pp. 25–36, 2015.

[32] S. K. Kopparapu, “Lighting design for machine vision application,” *Image Vis. Comput.*, vol. 24, no. 7, pp. 720–726, 2006.

[33] E. Tournas and M. Tsakiri, “Distance Error Estimation for Range Imaging Sensors,” *Archives*, vol. XXXVIII, 2010.

UNIVERSITI TEKNIKAL MALAYSIA MELAKA

APPENDICES

APPENDIX A ROBERTS EDGE DETECTION CODE

```
%% Image Acquisition
    img = snapshot(mycam);
    figure(1);
    imshow(img);
    title('Original')
% ROI generation
    c = [100 100 645 645];
    r = [405 955 955 405];
    BW = roipoly(img,r,c);
    [R, C]=size(BW);

    for i=1:R
        for j=1:C
            Out(i,j)=img(i,j);
       end
    end

    figure(2);
    imshow(Out,[]);
    title('ROI')
% Roberts Edge Detection
    BW1=edge(Out,'roberts',0.14);
    figure(3)
    imshow(BW1)
    title('Roberts Edge Detector')
% Removing unwanted outer edges
    c1 = [106 459 639 289];
    r1 = [789 942 576 415];
    BW3 = roipoly(BW1,r1,c1);
    [R1, C1]=size(BW3);

    for i1=1:R1
          for j1=1:C1
              if BW3(i1,j1)==1
               Out1(i1,j1)=BW1(i1,j1);
              else
               Out1(i1,j1)=0;
              end
          end
    end

    figure(4);
    imshow(Out1,[]);
    title('Removed Unwanted Edges')
% Dilation
    se = strel('square',20);
    BW4 = imdilate(Out1,se);
    figure(5);
    imshow(BW4);
    title('Dilated Image')
% Skeletonization and branch pruning
    skel= bwmorph(BW4,'skel',Inf);
    Out2 = bwmorph(skel, 'branchpoints');
```

UNIVERSITI TEKNIKAL MALAYSIA MELAKA

```
    E = bwmorph(skel, 'endpoints');
    [y,x] = find(E);
    B_loc = find(Out2);
    Dmask = false(size(skel));

    for k = 1:numel(x)
    D = bwdistgeodesic(skel,x(k),y(k));
    distanceToBranchPt = min(D(B_loc));
    Dmask(D < distanceToBranchPt) =true;
    end

    skelD = skel - Dmask;
    figure(6);
    imshow(skelD);
    title('Skeletonized & Pruned Branch Image')
% Smoothing / removing jagged corners
    dilatedImage = imdilate(skelD,strel('square',10));
    BW5 = bwmorph(dilatedImage,'thin',inf);
    figure(7);
    imshow(BW5);
    title('Thinned Image')
% Corner Detection
    C = detectMinEigenFeatures(BW5,'MinQuality', 0.3);
    figure(9)
    imshow(BW5)
    hold on
    plot(C.selectStrongest(4));
    title('Detected Points')
% Edge Detected over Original Picture
      figure(8)
      imshow(labeloverlay(img,BW5,'Colormap',[0 1
0],'Transparency',0));
      title('Edge Detected')
```

UTeM
اونيۏرسيتي تيکنيکل مليسيا ملاک
UNIVERSITI TEKNIKAL MALAYSIA MELAKA

APPENDIX B SOBEL EDGE DETECTION CODE

```
%% Image Acquisition
    img = snapshot(mycam);
    figure(1);
    imshow(img);
    title('Original')
% ROI generation
    c = [100 100 645 645];
    r = [405 955 955 405];
    BW = roipoly(img,r,c);
    [R, C]=size(BW);

    for i=1:R
        for j=1:C
            Out(i,j)=img(i,j);
       end
    end

    figure(2);
    imshow(Out,[]);
    title('ROI')
%   Sobel Edge Detection
    BW1=edge(Out,'sobel',0.14);
    figure (3)
    imshow(BW1)
    title('Sobel Edge Detection')
% Removing unwanted outer edges
    c1 = [106 459 639 289];
    r1 = [789 942 576 415];
    BW3 = roipoly(BW1,r1,c1);
    [R1, C1]=size(BW3);

    for i1=1:R1
          for j1=1:C1
            if BW3(i1,j1)==1
                Out1(i1,j1)=BW1(i1,j1);
            else
                Out1(i1,j1)=0;
            end
        end
    end

    figure(4);
    imshow(Out1,[]);
    title('Removed Unwanted Edges')
% Dilation
    se = strel('square',10);
    BW4 = imdilate(Out1,se);
    figure(5);
    imshow(BW4);
    title('Dilated Image')
% Skeletonization and branch pruning
    skel= bwmorph(BW4,'skel',Inf);
    Out2 = bwmorph(skel, 'branchpoints');
    E = bwmorph(skel, 'endpoints');
    [y,x] = find(E);
    B_loc = find(Out2);
    Dmask = false(size(skel));
```

UNIVERSITI TEKNIKAL MALAYSIA MELAKA

```
    for k = 1:numel(x)
    D = bwdistgeodesic(skel,x(k),y(k));
    distanceToBranchPt = min(D(B_loc));
    Dmask(D < distanceToBranchPt) =true;
    end

    skelD = skel - Dmask;
    figure(6);
    imshow(skelD);
    title('Skeletonized & Pruned Branch Image')
% Smoothing / removing jagged corners
    dilatedImage = imdilate(skelD,strel('square',10));
    BW5 = bwmorph(dilatedImage,'thin',inf);
    figure(7);
    imshow(BW5);
    title('Thinned Image')
% Corner Detection
    C = detectMinEigenFeatures(BW5,'MinQuality', 0.3);
    figure(9)
    imshow(BW5)
    hold on
    plot(C.selectStrongest(4));
    title('Detected Points')
% Edge Detected over Original Picture
    figure(8)
    imshow(labeloverlay(img,BW5,'Colormap',[0 1
0],'Transparency',0));
    title('Edge Detected')
```

UTeM
اونيۏرسيتي تيکنيکل مليسيا ملاک
UNIVERSITI TEKNIKAL MALAYSIA MELAKA

APPENDIX C PREWITT EDGE DETECTION CODE

```
%% Image Acquisition
    img = snapshot(mycam);
    figure(1);
    imshow(img);
    title('Original')
% ROI generation
    c = [100 100 645 645];
    r = [405 955 955 405];
    BW = roipoly(img,r,c);
    [R, C]=size(BW);

    for i=1:R
        for j=1:C
            Out(i,j)=img(i,j);
       end
    end

    figure(2);
    imshow(Out,[]);
    title('ROI')
%   Prewitt Edge Detection
    BW1=edge(Out,'prewitt',0.14);
    figure (3)
    imshow(BW1)
    title('Prewitt Edge Detection')
% Removing unwanted outer edges
    c1 = [106 459 639 289];
    r1 = [789 942 576 415];
    BW3 = roipoly(BW1,r1,c1);
    [R1, C1]=size(BW3);

    for i1=1:R1
        for j1=1:C1
            if BW3(i1,j1)==1
                Out1(i1,j1)=BW1(i1,j1);
            else
                Out1(i1,j1)=0;
            end
        end
    end

    figure(4);
    imshow(Out1,[]);
    title('Removed Unwanted Edges')
% Dilation
    se = strel('square',10);
    BW4 = imdilate(Out1,se);
    figure(5);
    imshow(BW4);
    title('Dilated Image')
% Skeletonization and branch pruning
    skel= bwmorph(BW4,'skel',Inf);
    Out2 = bwmorph(skel, 'branchpoints');
    E = bwmorph(skel, 'endpoints');
    [y,x] = find(E);
    B_loc = find(Out2);
    Dmask = false(size(skel));
```

UNIVERSITI TEKNIKAL MALAYSIA MELAKA

```
    for k = 1:numel(x)
    D = bwdistgeodesic(skel,x(k),y(k));
    distanceToBranchPt = min(D(B_loc));
    Dmask(D < distanceToBranchPt) =true;
    end

    skelD = skel - Dmask;
    figure(6);
    imshow(skelD);
    title('Skeletonized & Pruned Branch Image')
% Smoothing / removing jagged corners
    dilatedImage = imdilate(skelD,strel('square',10));
    BW5 = bwmorph(dilatedImage,'thin',inf);
    figure(7);
    imshow(BW5);
    title('Thinned Image')
% Corner Detection
    C = detectMinEigenFeatures(BW5,'MinQuality', 0.3);
    figure(9)
    imshow(BW5)
    hold on
    plot(C.selectStrongest(4));
    title('Detected Points')
  % Edge Detected over Original Picture
    figure(8)
    imshow(labeloverlay(img,BW5,'Colormap',[0 1
0],'Transparency',0));
    title('Edge Detected')
```

UTeM
اونيۏرسيتي تيکنيکل مليسيا ملاک
UNIVERSITI TEKNIKAL MALAYSIA MELAKA

APPENDIX D CANNY EDGE DETECTION CODE

```
%% Image Acquisition
    img = snapshot(mycam);
    figure(1);
    imshow(img);
    title('Original')
% ROI generation
    c = [100 100 645 645];
    r = [405 955 955 405];
    BW = roipoly(img,r,c);
    [R, C]=size(BW);

    for i=1:R
        for j=1:C
            Out(i,j)=img(i,j);
       end
    end

    figure(2);
    imshow(Out,[]);
    title('ROI')
% Canny Edge Detection
    BW1=edge(Out,'canny',[0 0.6]);
    figure(3)
    imshow(BW1)
    title('Canny Edge Detector')
% Removing unwanted outer edges
    c1 = [106 459 639 289];
    r1 = [789 942 576 415];
    BW3 = roipoly(BW1,r1,c1);
    [R1, C1]=size(BW3);

    for i1=1:R1
        for j1=1:C1
            if BW3(i1,j1)==1
                Out1(i1,j1)=BW1(i1,j1);
            else
                Out1(i1,j1)=0;
            end
        end
    end

    figure(4);
    imshow(Out1,[]);
    title('Removed Unwanted Edges')
% Dilation
    se = strel('square',10);
    BW4 = imdilate(Out1,se);
    figure(5);
    imshow(BW4);
    title('Dilated Image')
% Skeletonization and branch pruning
    skel= bwmorph(BW4,'skel',Inf);
    Out2 = bwmorph(skel, 'branchpoints');
    E = bwmorph(skel, 'endpoints');
    [y,x] = find(E);
    B_loc = find(Out2);
    Dmask = false(size(skel));
```

UNIVERSITI TEKNIKAL MALAYSIA MELAKA

```
    for k = 1:numel(x)
    D = bwdistgeodesic(skel,x(k),y(k));
    distanceToBranchPt = min(D(B_loc));
    Dmask(D < distanceToBranchPt) =true;
    end

    skelD = skel - Dmask;
    figure(6);
    imshow(skelD);
    title('Skeletonized & Pruned Branch Image')
% Smoothing / removing jagged corners
    dilatedImage = imdilate(skelD,strel('square',10));
    BW5 = bwmorph(dilatedImage,'thin',inf);
    figure(7);
    imshow(BW5);
    title('Thinned Image')
% Corner Detection
    C = detectMinEigenFeatures(BW5,'MinQuality', 0.3);
    figure(9)
    imshow(BW5)
    hold on
    plot(C.selectStrongest(4));
    title('Detected Points')
 %  Edge Detected over Original Picture
      figure(8)
      imshow(labeloverlay(img,BW5,'Colormap',[0 1
0],'Transparency',0));
      title('Edge Detected')
```

UTeM
اونيۏرسيتي تيکنيکل مليسيا ملاک
UNIVERSITI TEKNIKAL MALAYSIA MELAKA